REPORT DOCUMENTATION PAGE

Form Approved
OMB No. 0704-0188

1. AGENCY USE ONLY (Leave Blank)	2. REPORT DATE	3. REPORT TYPE AND DATES COVERED
	MAY 1990	THESIS - MS

4. TITLE AND SUBTITLE
THE DEVELOPMENT OF AN INTEGRATING CAVITY ABSORPTION METER TO MEASURE OPTICAL ABSORPTION OF PURE WATERS AND SUSPENDED PARTICULATES

5. FUNDING NUMBERS

6. AUTHOR(S)
ROBIN MERL POPE

7. PERFORMING ORGANIZATION NAME(S) AND ADDRESS(ES)
TEXAS A&M UNIVERSITY
DEPARTMENT OF PHYSICS

8. PERFORMING ORGANIZATION REPORT NUMBER

9. SPONSORING/MONITORING AGENCY NAME(S) AND ADDRESS(ES)
HQDA
MILPERCEN (DAPC-OPB-O)
ALEX, VA 22332-0411

10. SPONSORING/MONITORING AGENCY REPORT NUMBER

11. SUPPLEMENTARY NOTES

12a. DISTRIBUTION/AVAILABILITY STATEMENT
UNLIMITED

12b. DISTRIBUTION CODE

13. ABSTRACT (Maximum 200 words)

THE INTEGRATING CAVITY ABSORPTION METER (ICAM) PROVIDES AN INSTRUMENT CAPABLE OF MEASURING OPTICAL ABSORPTION INDEPENDENT OF SCATTERING EFFECTS. THE THEORY OF THE DEVICE IS REVIEWED, THE INSTRUMENT IS DESCRIBED, AND MEASURMENT RESULTS ARE PRESENTED FOR: ABSORPTION RESULTS IN THE PRESENCE OF VARYING CONCENTRATIONS OF SCATTERERS; ABSORPTION SPECTRA OF VARIOUS PURE WATER SAMPLES COMPARED TO ACCEPTED VALUES; AND ABSORPTION SPECTRA FOR VARIOUS PHYTOPLANKTON CULTURES.

14. SUBJECT TERMS	15. NUMBER OF PAGES
OPTICAL ABSORPTION; ISOTROPIC ILLUMINATION, INTEGRATING CAVITY; SCATTERING, LIGHT,	54
	16. PRICE CODE

17. SECURITY CLASSIFICATION OF REPORT	18. SECURITY CLASSIFICATION OF THIS PAGE	19. SECURITY CLASSIFICATION OF ABSTRACT	20. LIMITATION OF ABSTRACT
UNCLASSIFIED	UNCLASSIFIED	UNCLASSIFIED	UL

(2)

THE DEVELOPMENT OF AN INTEGRATING CAVITY ABSORPTION METER TO MEASURE OPTICAL ABSORPTION OF PURE WATERS AND SUSPENDED PARTICULATES

A Thesis

by

ROBIN MERL POPE

Submitted to the Office of Graduate Studies of
Texas A&M University
in partial fulfillment of the requirements for the degree of

MASTER OF SCIENCE

May 1990

Major Subject: Physics

THE DEVELOPMENT OF AN INTEGRATING CAVITY ABSORPTION METER TO MEASURE OPTICAL ABSORPTION OF PURE WATERS AND SUSPENDED PARTICULATES

A Thesis

by

ROBIN MERL POPE

Approved as to style and content by:

Edward S. Fry
(Chair of Committee)

Norman L. Guinasso Jr.
(Member)

George W. Kattawar
(Member)

Richard L. Arnowitt
(Head of Department)

May 1990

ABSTRACT

The Development of an Integrating Cavity Absorption Meter to Measure Optical Absorption of Pure Waters and Suspended Particulates. (May 1990)

Robin Merl Pope, B.S., United States Military Academy

Chair of Advisory Committee: Dr. Edward S. Fry

The Integrating Cavity Absorption Meter (ICAM) provides an instrument capable of measuring optical absorption independent of scattering effects. The measurement of optical absorption has always been complicated by scattering effects. The most common and perhaps simplest method of measuring absorption is based on transmission of light through the sample. Scatterers produce systematic errors which prevent simple transmission type absorption measurements. The ICAM is, in principal, rigorously independent of scattering effects. In this thesis ~~paper~~ the theory of the device is reviewed, and five developmental models of the device are described. Measurement results are presented for: absorption results in the presence of varying concentrations of scatterers; absorption spectra of various pure water samples compared to accepted values; and absorption spectra for various phytoplankton cultures. Absorption values as low as .001 meters^{-1} have been measured.

Keywords: Optical absorption, Isotropic illumination, Light scattering, Theses. (LDC)

TABLE OF CONTENTS

CHAPTER		Page
I	INTRODUCTION	1
II	REVIEW OF LITERATURE	2
III	THEORY	4
IV	EXPERIMENTAL APPARATUS	9
	A Model I	11
	B Model II	13
	C Model III	15
	D Model IV	16
	E Model V	17
V	CALIBRATION	19
VI	MEASUREMENT RESULTS	24
	A Independence of Scattering	24
	B Linearity	29
	C Spectral Measurements	30
	D Energy Density Within the Sample	41
VII	CONCLUSION	45
REFERENCES		46
VITA		48

LIST OF FIGURES

FIGURE		Page
1	Cross Section of the integrating cavity system .	5
2	Schematic of the ICAM system	10
3	Model I cross section parallel to the Z-axis . .	12
4	Model I cross section transverse to the Z-axis .	13
5	Model II cross section parallel to the Z-axis . .	14
6	Model II cross section transverse to the Z-axis .	14
7	Model III cross section parallel to the Z-axis . .	16
8	Model IV cross section parallel to the Z-axis . .	17
9	Model V cross section parallel to the Z-axis . .	18
10	Model V cross section transverse to the Z-axis .	18
11	Absorption of Irgalan Black samples measured in a Cary 219 spectrophotometer	19
12	Absorption vs the ratio (S1/S0) at 630 nm . .	20
13	(S1/S0) vs volume for fixed sample absorption .	23
14	Observed absorption of water at 630 nm versus concentration of nonabsorbing scatterers in models II and V	25
15	Irradiance vs distance from sample boundary . .	28
16	Linearity test; absorption versus dye concentration	29
17	Absorption spectra for seawater, seawater filtrate, and distilled water	32
18	Absorption spectra for seawater particulates . .	33
19	Difference between seawater filtrate and distilled water	34

FIGURE		Page
20	Absorption spectra for *Dunaliella tertiolecta* . .	35
21	Absorption spectra for *Micromonas pusilla* . . .	36
22	Absorption spectra for various pure waters compared to data from Smith and Baker, 550 to 700 nm	38
23	Absorption spectra for various pure waters compared to data from Smith and Baker, 400 to 550 nm	39
24	Experimental apparatus to determine Kg(θ) . .	44

CHAPTER I

INTRODUCTION

Accurate measurement of the optical absorption coefficient for both pure and natural waters has been complicated by the effects of scattering particulates. E. S. Fry has proposed a method of measuring absorption which eliminates the systematic effects of scattering. This device, hereafter referred to as the Integrating Cavity Absorption Meter or ICAM, offers the advantages of being simple, rugged, and capable of in situ measurements. The theoretical basis is sound and well documented.[1] Five versions of the ICAM have been constructed, calibrated, and tested. Optical absorption spectra of pure water throughout the visible compare favorably with accepted values[2].

Journal model is Applied Optics

CHAPTER II

REVIEW OF LITERATURE

Methods of measuring optical absorption include: (1) carefully preparing a pure sample, usually by repeated distillation in quartz, and then passing a beam of light through a long tube filled with the sample[3] (2) measuring the attenuation of a beam of light passed through a long tube of water, then measuring the scattering coefficient of the water and mathematically determining the absorption coefficient[4] (3) Using a long tube with a highly reflecting lining to minimize scattering losses[5, 6] (4) Using a point source of radiation and measuring the attenuation at a given radial distance and over a known detector area, assuming scattering in the sample is isotropic[7] (5) placing the sample at the entrance window of an integrating cavity[8] (6)thermal lense or photothermal techniques based on the temperature dependance of the refractive index[9] (7)adiabatic laser calorimetry[10] (8) split-pulsed laser methods to measure extinction and scattering, an advanced version of (2) above,[11] (9) Optoacoustic techniques to measure sound waves produced by thermal expansion in a water column subjected to an incident light beam; the expansion depends on the radiation absorbed by the water.[12]

The concept of using an integrating cavity to aid in measuring absorption has been used by various researchers within the last two decades. Elterman described the use of an integrating sphere to measure optical absorption.[13] Integrating cavities have been used to

measure absorption of particles placed on the cavity floor, in suspension, or concentrated on filters.[14,15,16] Using a similar principal (isotropic radiation) A.D. Clark has developed a variation of the integrating plate method (also known as opal glass plate method) which he refers to as the integrating sandwich to enhance absorption effects of particulate matter deposited on glass filters.[17]

CHAPTER III

THEORY

The ICAM uses a system of integrating cavities to produce isotropic illumination of the sample.[1] To understand why the ICAM is independent of scattering, let us first consider the basic principle of a single integrating cavity.

The inside surface of a typical integrating cavity has a high diffuse reflectance (Lambertian). A beam of radiation introduced into the cavity and incident upon this Lambertian surface is diffusely reflected into all directions. After numerous reflections, the interior of the cavity is filled with a very uniform, isotropic radiance distribution. The radiance level is directly proportional to the total optical power introduced into the cavity. Any object placed inside the cavity will be uniformly illuminated from all directions. If nonabsorbing scatterers are placed in the cavity, the net irradiance incident on the wall of the cavity will remain unchanged. The cavity will contain the same amount of energy both before and after the addition of the scatterers; there is no loss of radiant energy due to scattering. Even if particles in the sample scatter radiation through some preferred angle, the Lambertian surface of the cavity will uniformly distribute the radiation so that the irradiance striking the wall of the cavity will be uniform. If the scatterers in the cavity have some characteristic absorption, the irradiance incident on the wall of the cavity will vary inversely with this absorption. By measuring this irradiance we can determine the absorption independent of scattering within the cavity.

In designing a system to produce isotropic illumination in an integrating cavity we want to avoid any bright spot at the point where light is introduced into the cavity and we want to avoid placing any object in the direct path of this input beam. We achieve this by using a system of integrating cavities and by careful selection of materials for construction of these cavities. Our system of integrating cavities consists of one cavity **A** completely contained within another **B** as shown in Figure 1.

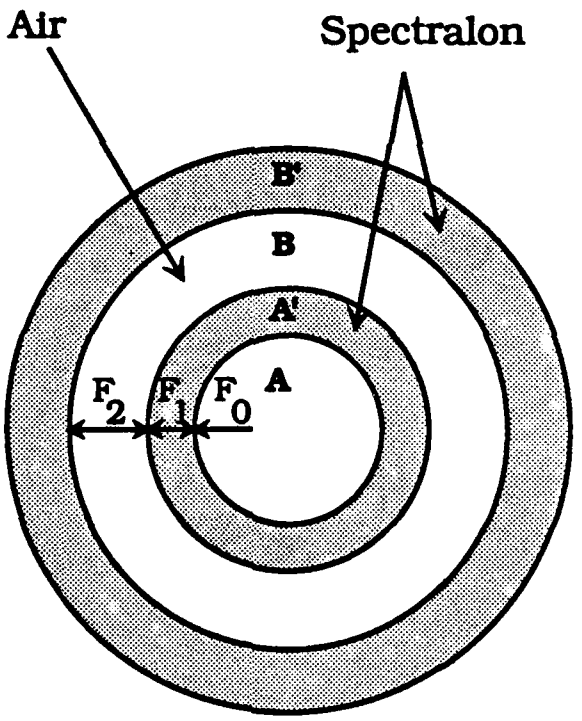

Figure 1. Cross section of the integrating cavity system. Our device has cylindrical symmetry about an axis perpendicular to the figure.

The cells **A'** and **B'** which constitute the walls of these cavities are made of Spectralon™, a material with very high diffuse reflectivity throughout the visible and which is easily machineable. Cavity **B** is an air space. We place our sample in cavity **A**. When light enters cavity **B** it will bounce between the two cell walls filling cavity **B** with isotropic radiation. Irradiance incident on the wall of cell **B'** from within **B** is designated F_2.

The Spectralon wall, **A'**, allows some portion of the incident radiation to pass through it and into cavity **A**. The portion of incident radiation that is transmitted is proportional to $(1-\rho)$, where ρ is the reflectivity of the wall. At each reflection, only a very small percentage of the incident light enters cavity **A**, but the radiation bounces around many times in cavity **B** and effectively "tries" many times so that the radiance in **A** builds up to an appreciable value. Since the wall **A'** is surrounded by a uniform radiance, light enters cell **A** and the sample from every direction thus avoiding any bright spot from a beam entering the cavity. This unique dual cavity design is one of the distinguishing features of this instrument.

Another important feature is the extremely long path length achieved inside the integrating cavity. In order to measure very small absorptions one must use a long path length through the sample. The high reflectivity of the integrating cavity wall produces a path length that is many times the cavity diameter. For an empty cavity with a wall reflectivity of .992 (the reflectivity of spectralon at 550 nm) light will reflect 125 times before reflection losses decrease the intensity by a factor of e^{-1}. For a cavity diameter of 3 cm this would produce a

path length of 3.75 meters and a diameter of 10 cm would produce a path length of 12.5 meters. It is easy to see that the high reflectivity of the cavity walls gives us a path length that will be sensitive to very small absorptions.

Assuming the radiance distribution within each integrating cavity to be isotropic and homogeneous, we denote the irradiance on the inner wall of cell **A'** from within **A** as F_0, and from within **A'** as F_1. If the absorption of the Spectralon and the sample was precisely zero, the equilibrium condition would be $F_2=F_1=F_0$. In practice this is not the case, but we can use conservation of energy to determine their relationships. At the boundary between cell **A'** and the sample in cavity **A** , it is clear that the energy entering the sample equals the energy leaving the sample plus energy absorbed by the sample[2],

Energy Supplied		Energy Lost Through Wall		Energy Lost Through Detector		Energy Absorbed	
$F_1A_0(1-\rho)$	=	$F_0A_0(1-\rho)$	+	F_0A_D	+	$4\alpha F_0V_0$.	(1)

where ρ denotes the reflectivity at the boundary (wavelength dependent), A_0 is the area of the boundary surface of cavity **A**, A_D is the area of the fiber optic detector for measuring F_0, V_0 denotes the volume of the sample, and α denotes the absorption coefficient of the sample. Solving this equation for the absorption coefficient gives,

$$\alpha = \frac{1}{4V_0}\left[\frac{F_1}{F_0}A_0(1-\rho) - \{A_0(1-\rho)+A_D\}\right]. \qquad (2)$$

Now the measured signals which are proportional to F_1 and F_0 are designated by S_1 and S_0, respectively. The ratio F_1/F_0 can then be replaced by S_1/S_0. If we now also note that for a fixed wavelength and volume, the parameters ρ, A_0, A_D, and V_0 are all constants, then we can write,

$$\alpha = K_1 \frac{S_1}{S_0} - K_2, \tag{3}$$

or, explicitly showing the dependence on V_0,

$$\alpha V_0 = K_3 \frac{S_1}{S_0} - K_4, \tag{4}$$

where, K_1, K_2, K_3, and K_4 are wavelength dependent calibration constants which must be experimentally determined.

Methods of determining the constants will be discussed in chapter V.

CHAPTER IV

EXPERIMENTAL APPARATUS

Figure 2 shows a schematic representation of the ICAM system. We use an Oriel model 66005 arc lamp system with a 150 watt Xenon lamp as our light source. A set of thirty-one 10nm bandwidth interference filters (1 filter every 10 nm from 400 to 700nm) determine the wavelength. Our light source is chopped by an EG&G Princeton Applied Research Model 197 light chopper. Six plastic optical fibers, 1.0 mm diameter, carry the light to the integrating cavities; three more fibers sample the irradiances F_0, F_1, and F_2. These latter fibers are coupled to Burle 4840 photomultiplier tubes which send current signals to a lock in amplifier referenced to the light chopper frequency. A Keithley 199 digital volt meter converts the analog voltages(S_0,S_1, and S_2) from the amplifier into digital signals and sends them via a IEEE-488 bus to a Macintosh II minicomputer. Using LabView software a virtual instrument then displays the value of the absorption coefficient.

Five variations of a system of integrating cavities have been produced and evaluated. These will be referenced as models I-V. This series of models provides a thorough understanding of the capabilities and limitations of the ICAM system. Therefore it is important to describe each model as well as its associated experimental results.

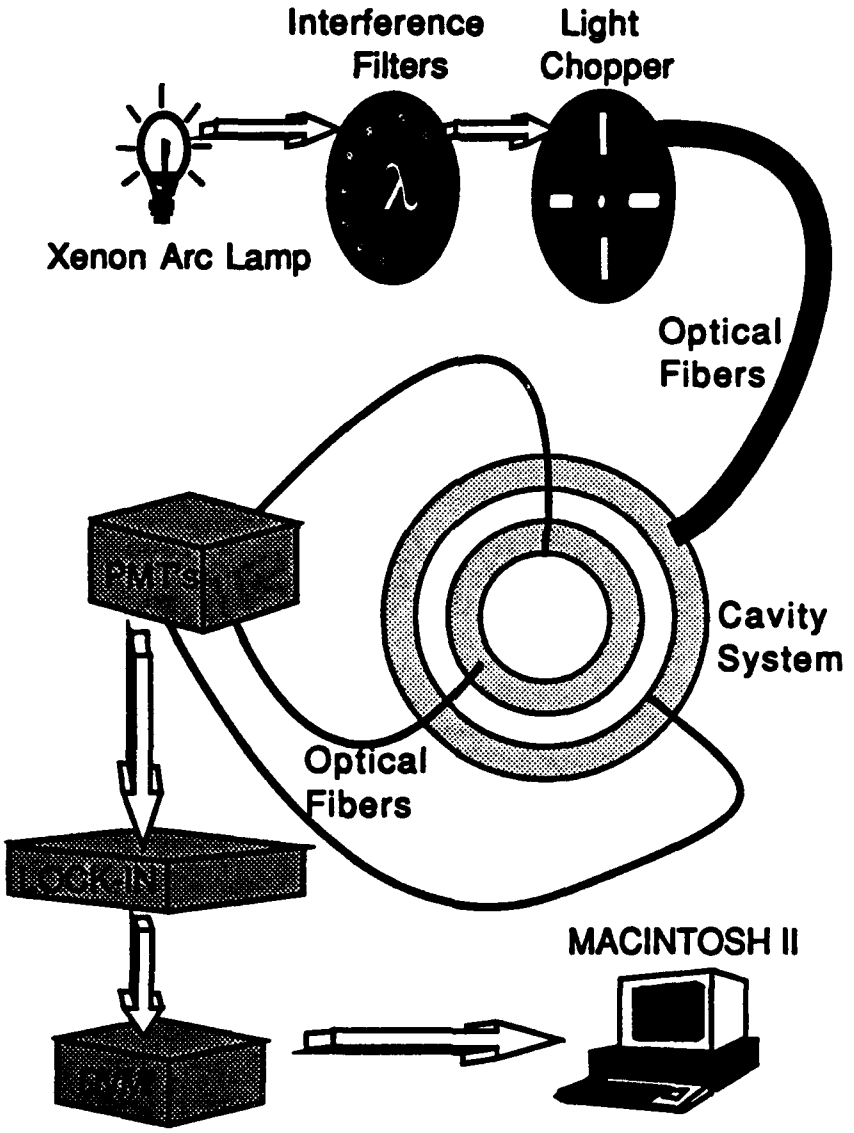

Figure 2. Schematic of the ICAM system.

A. Model I

Figures 3 and 4 show cross sections of the ICAM integrating cavities for model I. This system is rotationally symmetric about the Z-axis. The center cavity is made of Spectralon with a wall thickness of 6 mm, outer diameter of 5 cm, and length of 10 cm. The inner cavity holds an 83 ml. sample. The outer cavity is made of stainless steel with the inner surface coated with Duraflect™. The inside dimensions of the outer cavity provide a 1 cm space between the outer and inner cavities. Eight spectralon dowels support the inner cavity and position it in the center of the outer cavity. Six of these are positioned in the X-Y plane, and 2 are positioned along the Z-axis at each end of the inner cavity. Samples can be exchanged through a 3 mm diameter hole in the top of the cavity which runs through the upper supporting dowel. This exchange is accomplished using a long nosed pipet capable of reaching the bottom of the inner cavity. Six optical fibers supply light to the outer cavity. Three of these are positioned at each end of the system and they enter the cavity at an angle of 60 degrees from normal to the cavity wall in the Z direction. The optical fibers used to measure F_0, F_1, and F_2 are positioned at the midpoint of the cylinder axis and are symmetrically spaced every 120 degrees in the x-y plane (figure 4). The F_2 detector fiber terminates at the inner surface of **B'**. The F_1 detector fiber terminates at the midpoint of the inner wall, **A'**. The F_0 detector fiber terminates at the inner surface of **A'**. The F_0 and F_1 fibers are shielded from the F_2 irradiance by vinyl tubing which is then coated with a white silicone

glue. All 9 fibers are shielded by black vinyl tubing from the exterior of **B'** to their termination/origin.

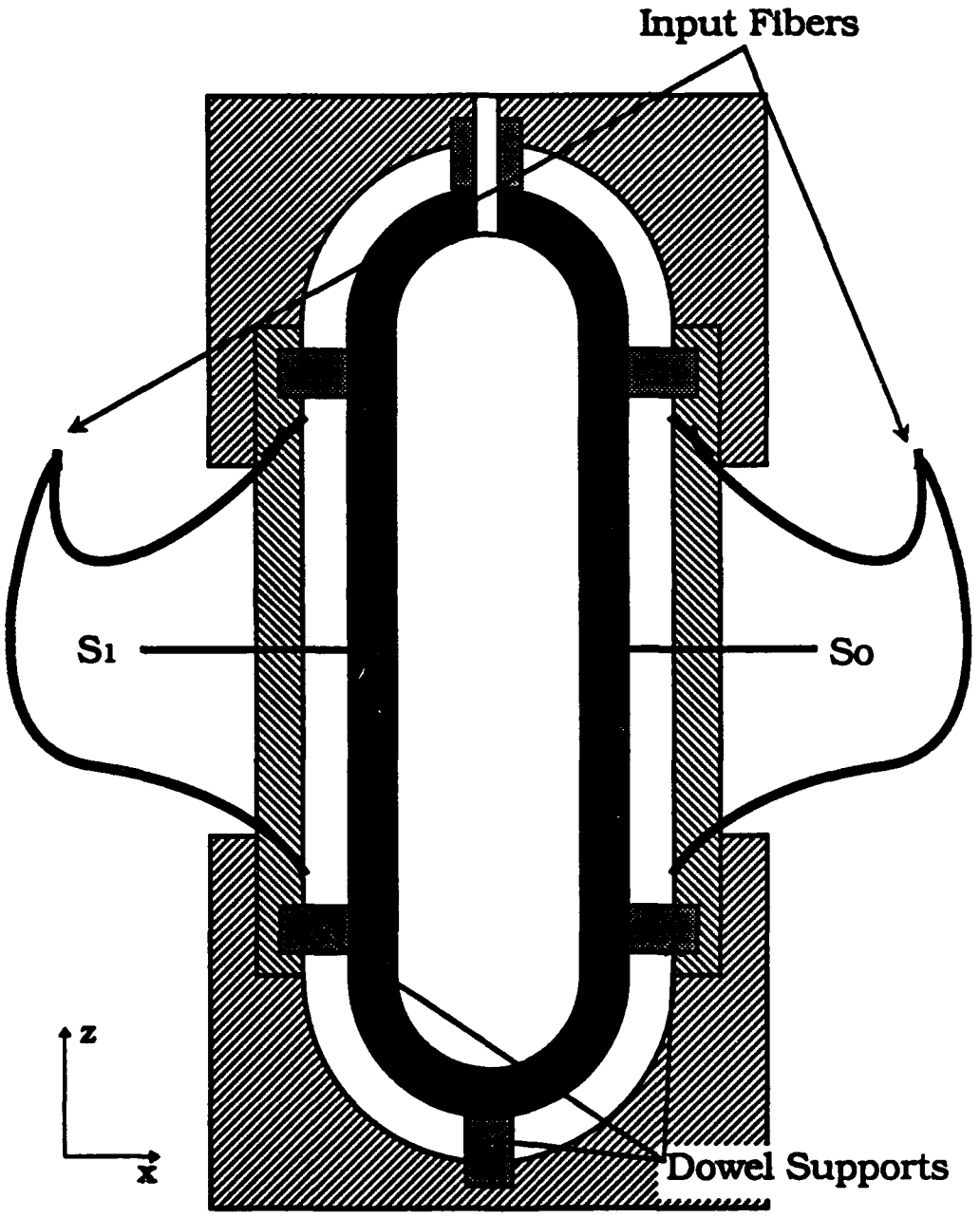

Figure 3. Model I cross section parallel to the Z-axis.

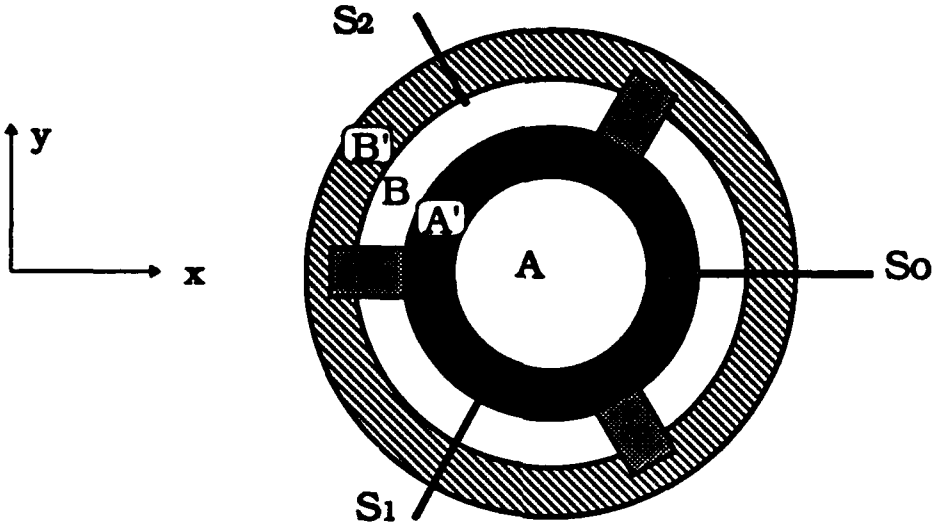

Figure 4. Model I cross section transverse to the Z-axis.

B. Model II

Figures 5 and 6 show cross sections of the ICAM integrating cavities for model II parallel and transverse to the Z-axis respectively. Both cavities are 15 cm long Spectralon cylinders. The outer cylinder is 10 cm in outer diameter with a 1.27 cm wall thickness. The inner cylinder is 5 cm in outer diameter and 6 mm wall thickness. Spectralon end caps seal the 2 cavities and hold the inner cell coaxially with respect to the outer cell (figure 5). Six input fibers from the arc lamp pass through the end caps and terminate in the outer cavity. The three fibers entering each end cap are 120 degrees apart on a 6.4 cm diameter circle and those at one end are offset by 60 degrees with respect to those at the other. The inner cavity is lined with a quartz bulb which tapers into quartz capillary tubing at each end. This permits the exchange of samples without opening the cavities and avoids direct contact between the Spectralon and the sample. This quartz bulb holds 118 ml.

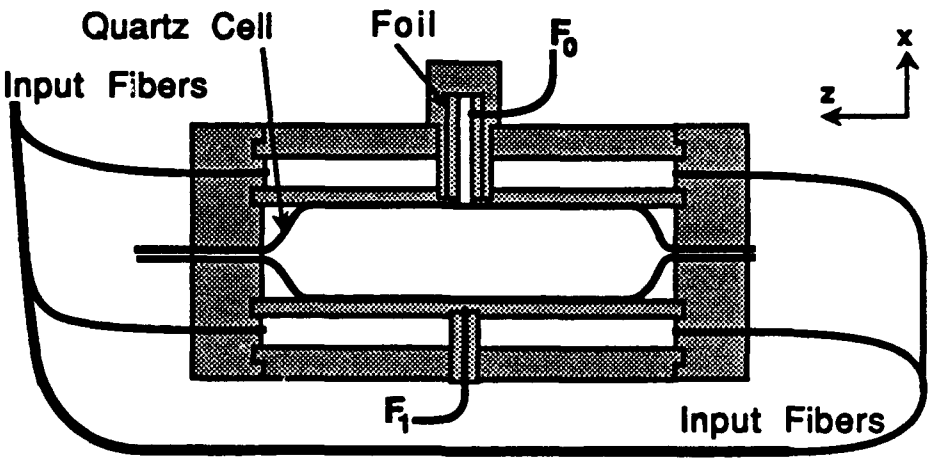

Figure 5. Model II cross section parallel to the Z-axis.

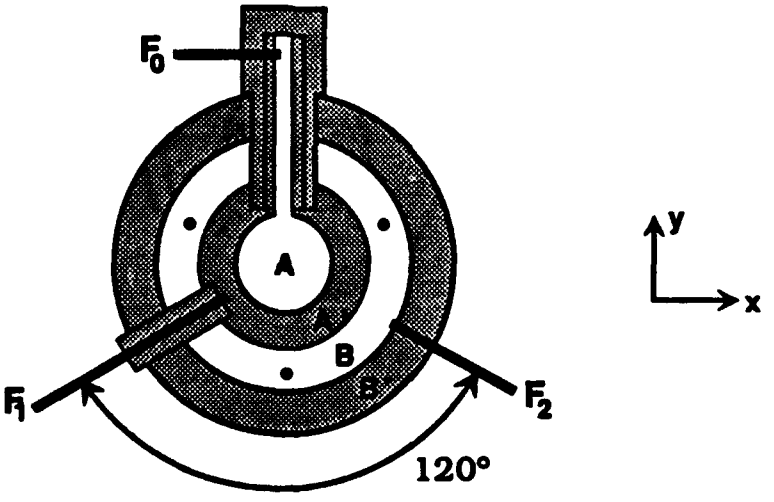

Figure 6. Model II cross section transverse to the Z-axis.

The optical fibers used to measure F_0, F_1, and F_2 are positioned at the midpoint of the cylinder axis and are symmetrically spaced every 120 degrees in the x-y plane (figure 6). The F_2 detector fiber terminates at the inner surface of **B'**. The F_1 detector fiber terminates at the midpoint of the inner wall, **A'**. This fiber is isolated from the radiances in cavity **B** and in the wall **B'**, by wrapping the fiber with aluminum foil and then inserting it into a 3/8" OD Spectralon tube. To measure the irradiance from within the sample cavity, **A**, a tube of Spectralon with 1/4" ID and 3/8" OD is inserted into the side of the cavity. A detector fiber at the end of this tube gives a signal proportional to the required irradiance. To prevent the radiances in **A'**, **B**, and **B'** from penetrating this tube we shield it with aluminum foil and then surround it with another Spectralon tube 3/8"ID by 3/4" OD. The outer Spectralon tube prevents the foil shielding from appreciably perturbing these radiances. This system is placed in a light-tight enclosure and the photomultiplier tubes are mounted directly on the sides of the enclosure. All 9 fibers are shielded between the outside wall of **B'** and their termination/origin points as in model I.

C. Model III

Model III is the same design as model II with the exception that the diameter of the quartz bulb is 2.54 cm leaving a air gap of approximately .6 cm between it and the inner wall of the inner cylinder. This quartz bulb holds 75 ml. Figure 7.

D. Model IV

Model IV is identical to model III with the exception of a 1.27 cm long band (or ring) made of spectralon positioned around the midpoint of the quartz bulb. This band is approximately 3 mm thick at its midpoint and tapers toward each end. Figure 8.

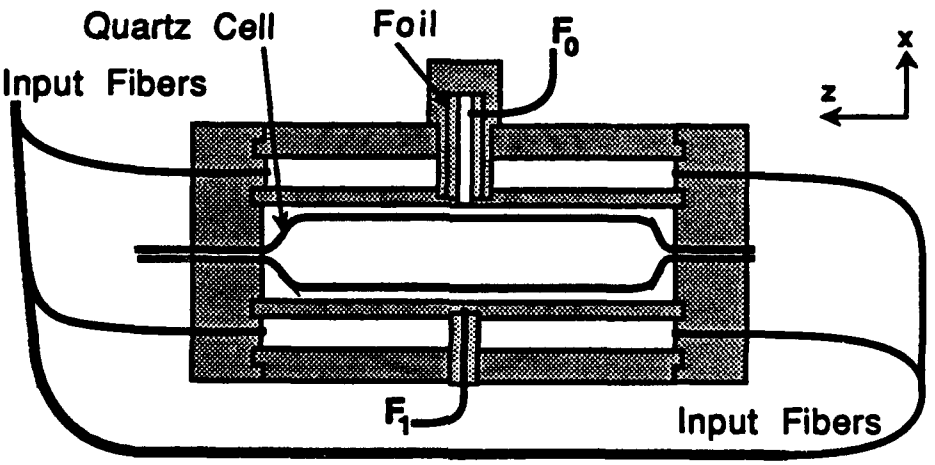

Figure 7. Model III cross section parallel to the Z-axis.

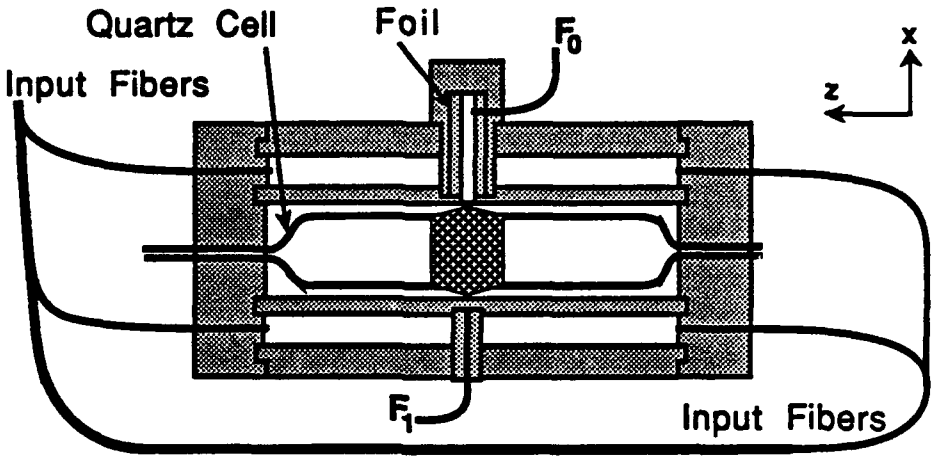

Figure 8. Model IV cross section parallel to the Z-axis.

E. Model V

Model V is shown in figures 9 and 10. This model was designed to hold a sample volume of 615 ml. in a quartz glass bulb similar to the one described in system II. The inner and outer cavities are made of spectralon. The outer cavity is 1.27 cm thick, 25.4 cm long, and has a hexagonal cross section when viewed along the z-axis. The inner cavity is a cylinder 6 mm thick, 16 cm long and 10 cm in diameter. The inner cavity is held at the midpoint of the outer cavity by spectralon tubes of 2.54 cm OD, 8 mm ID and 5 cm long positioned at each end of the system. Three spectralon dowels at each end of the cavity 8 mm in diameter by 5 cm long help stabilize the inner cavity. Input and detector fibers are positioned and shielded as described in model II.

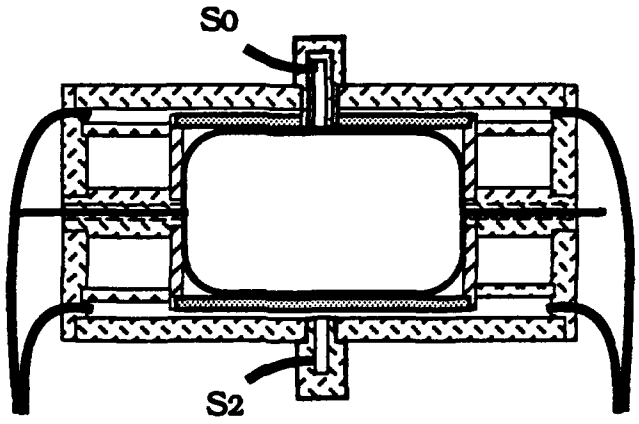

Figure 9. Model V cross section parallel to the Z-axis.

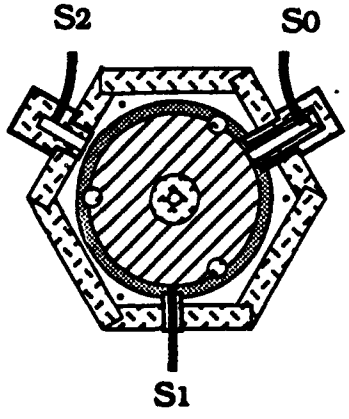

Figure 10. Model V cross section transverse to the Z-axis.

CHAPTER V

CALIBRATION

Two methods of determining the calibration constants have been used. We can prepare several samples containing varying concentrations of an absorbing pigment or dye. A spectrophotometer is then used to determine the absorption of the dye. The dye selected for this procedure was Irgalan Black™ (Ciba-Geigy Corp.) due to its fairly constant absorption throughout the spectrum of interest. Figure 11 shows the absorption results for various samples measured in a Cary model 219 spectrophotometer. The spectrophotometer

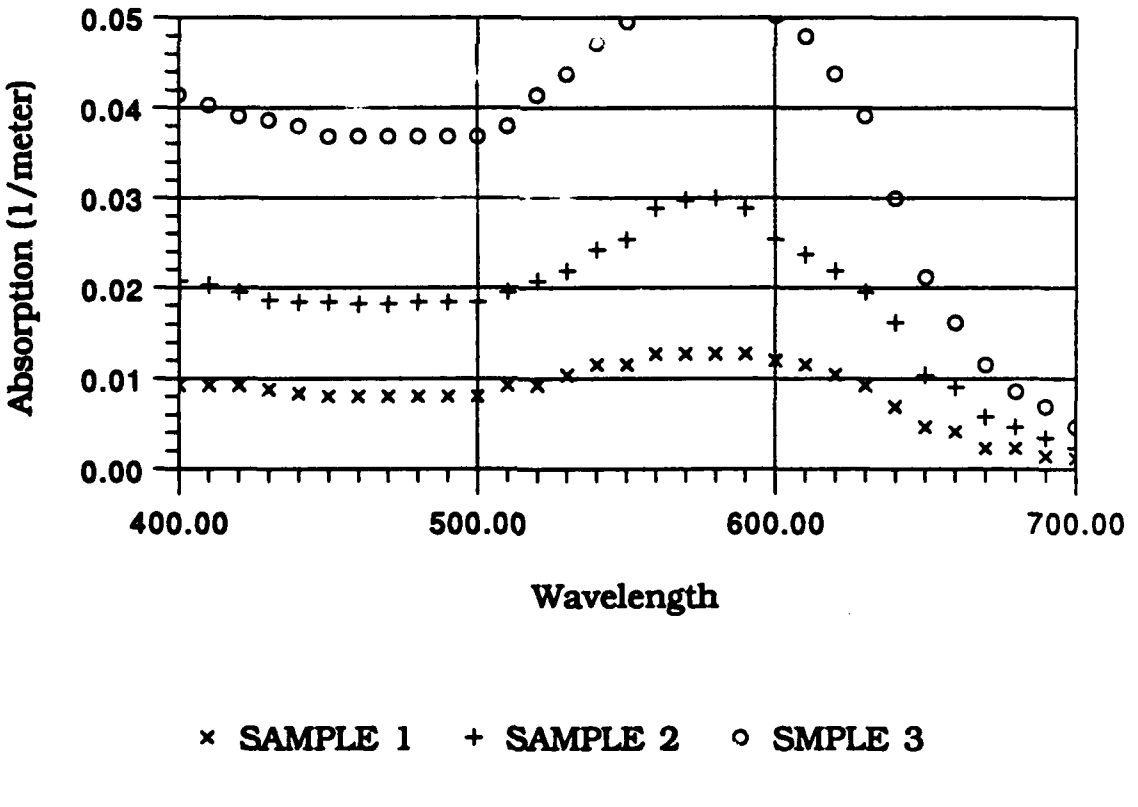

Figure 11. Absorption of Irgalan Black samples measured in a Cary 219 spectrophotometer.

measures the absorption of the dye relative to a sample containing pure water with no dye, therefore we do not know the total absorption of these samples (Total absorption = absorption of dye + absorption of water) but we do know the change in absorption between each of the samples. When placed in the ICAM each of these samples will produce a unique value for the ratio (S_1/S_0) By plotting the change in absorption vs (S_1/S_0) and using the method of least squares fit, we can determine the value for K_1 of equation (3) as the slope of the line fitted to these points. Figure 12 shows the results of this method at a wavelength of 630 nm. Note that as the dye

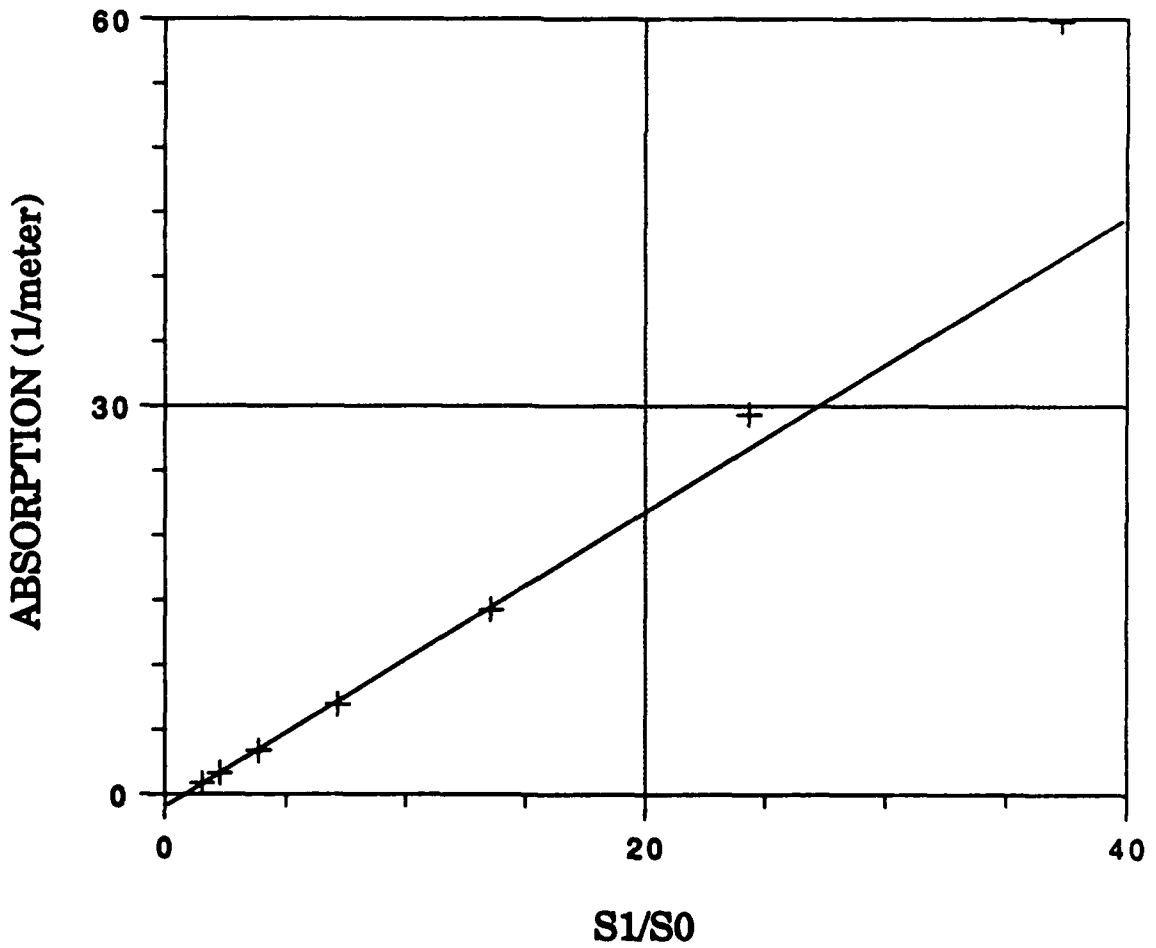

Figure 12. Absorption vs the ratio (S_1/S_0) at 630 nm.

concentration increases the S_0 signal will decrease linearly. At sufficiently high dye concentrations the absorption in the sample is so large that the radiation distribution becomes anisotropic and the decrease becomes non-linear. Specifically, the energy density decreases towards the center of the sample (photons have a high probability of absorption before reaching the center). This results in absorption becoming a nonlinear function of (S_1/S_0) as noted at the extreme right data point in figure 12. This information also establishes the dynamic range for the ICAM as the absorption range that is linear with respect to (S_1/S_0). After values for K_1 have been determined, we must determine the intercept value (K_2) for equation (3). To fix the intercept we must have one sample where the total absorption is known. We measure the value of (S_1/S_0) with the cavity empty and set the absorption equal to zero. We can then solve equation (3) for K_2. The procedure just described assumes the optical properties of the ICAM do not change appreciably when the index of refraction within the sample volume changes.

By determining the intercept with the cavity empty, the meter will measure the total absorption of any solution/suspension placed in cell A. The absorption of suspended particulates can be determined by measuring the sample with the particles in suspension, filtering the solution to remove the particles, and then measuring the filtrate. Subtracting the filtrate absorption from the suspension absorption will give the absorption of the particulate matter only.

It should be noted that for measuring the absorption of suspended particulate matter or dissolved substances, where the absorption of the

filtrate must be subtracted from the total absorption within the cavity, the calibration procedure can be simplified. We can set the absorption of the filtrate to zero (provided the calibration samples use the same medium). This allows both K_1, and K_2 to be determined from the best fit of absorption vs S_1/S_0 for the calibration samples where one sample contains pure medium (no added pigment). The absorption measured in the ICAM under these constraints will be only the absorption of the suspended particulate matter. This is equivalent to determining a baseline when using a spectrophotometer. We then measure absorptions compared to the baseline. The ICAM offers the ability to measure absorption of suspended particulates as well as the absolute absorption of the medium, both of which are not possible in a spectrophotometer.

In this work, calibration was also accomplished using only one solution whose absorption was accurately determined with a spectrophotometer. Figure 13 shows the measured ratio, S_1/S_0, as a function of the volume of this solution in the sample cavity. A least squares procedure was used to fit this data to a straight line and the calibration constants were determined from the values of the slope and intercept using equations (3) and (4).

This latter calibration procedure is not generally used because it introduces an air-liquid interface within the sample volume and the position of this interface changes every time the volume is changed. The preferred method (setting the absorption equal to zero with the cavity empty and using several

samples of varying absorption) always fills the sample volume with one homogeneous sample.

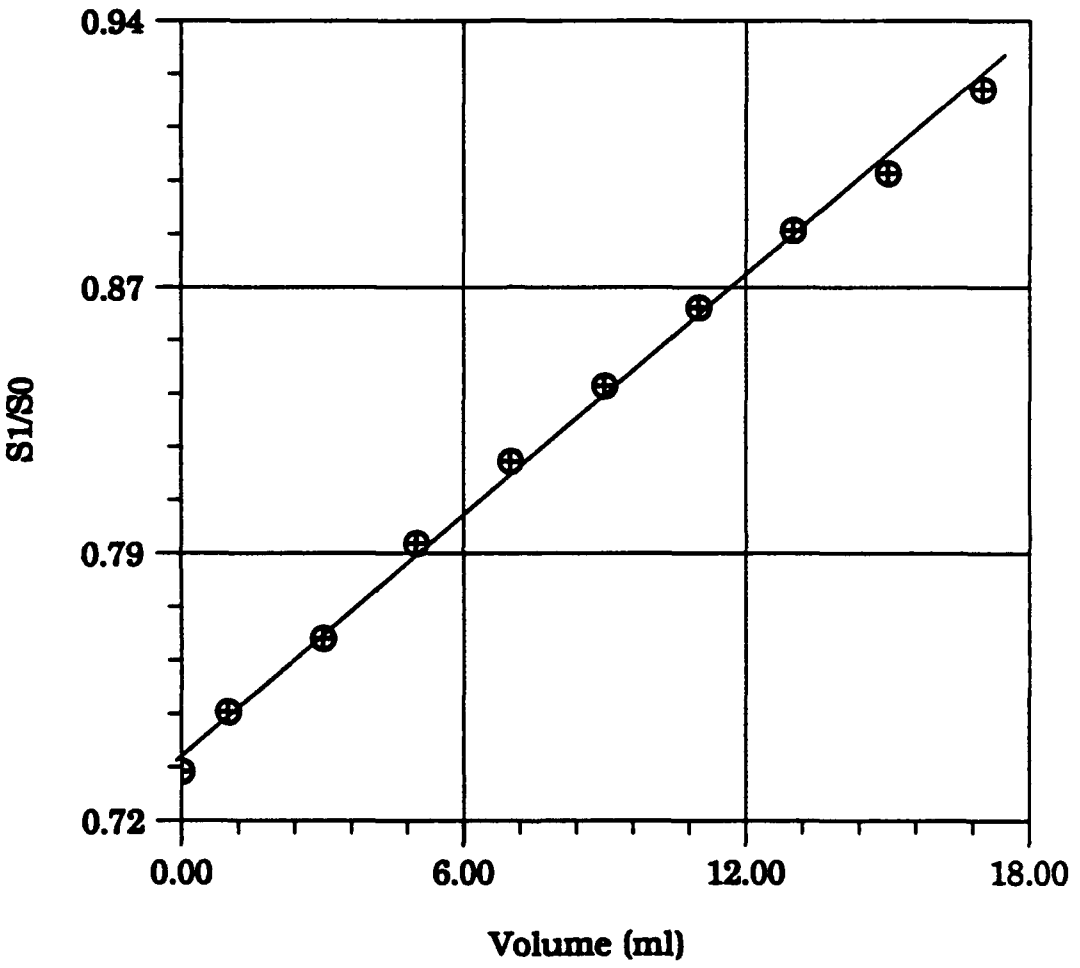

Figure 13. (S_1/S_0) vs volume for fixed sample absorption.

CHAPTER VI

MEASUREMENT RESULTS

A. Independence of Scattering

Of greatest importance is the effect on the observed absorption produced by the addition of nonabsorbing scattering particulates to the sample. Magnesium Oxide was used for some of the early studies conducted with model I. The MgO was abandoned due to its solubility in water and lack of accurate absorption data for MgO in the visible. Quartz powder was selected as a better alternative for the scattering particles. The particles are irregular and of the order of 0.5 to 10 microns in dimensions. They remain suspended in the water for the duration of the absorption measurements. The measured absorption of water at 630 nm as a function of increasing concentrations of scatterers using models II and V is shown in figure 14. Table 1 shows the scattering coefficient for each quartz concentration of figure 14. For these measurements the calibration constants K_1 and K_2 were (0.5197 m^{-1} and 0.8642 m^{-1}) for model II and (0.6715 m^{-1} and 0.5901 m^{-1}) for model V. This measured absorption shows an anomalous increase with increasing concentration of scatterers beyond ≈1 gm/l. However, the effect is small; even at 2.3 gm/l the measured absorption is only in error by ≈15%. At 1 gm/l, where the scattering has negligible effect, the extinction length due to scattering is only about 7 cm. Since the cavity diameter of model II is 3.7 cm, the corresponding scattering optical depth is 0.53. At the same time, due to the high reflectivity of the walls and the corresponding large number

of transits through the sample, the effective extinction length due to absorption by the water is ≈3.7 m.

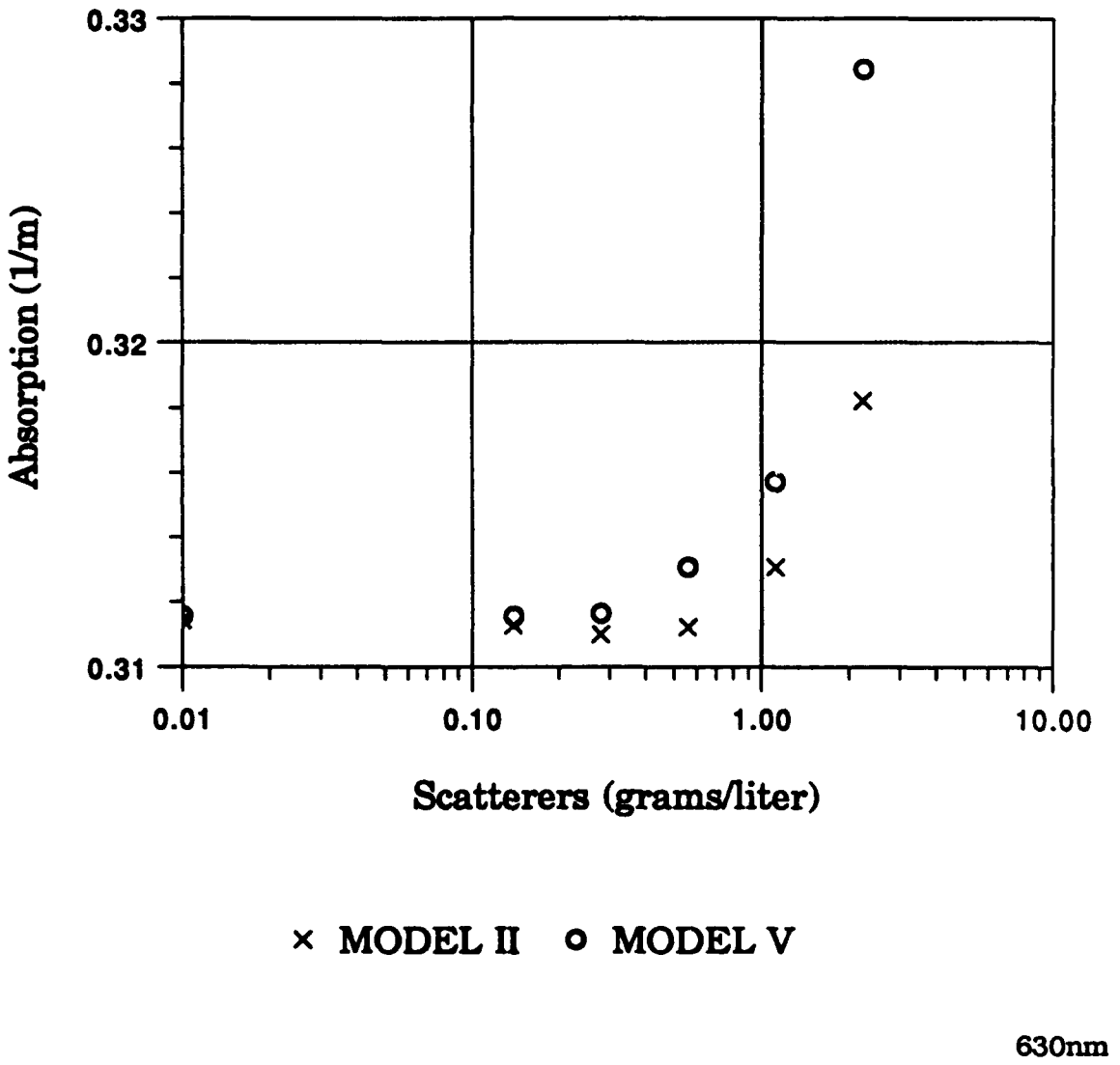

Figure 14. Observed absorption of water at 630 nm versus concentration of nonabsorbing scatterers in models II and V.

Table 1. Scattering coefficients for various concentrations of quartz powder suspended in pure water.

Scatterers (grams/liter)	Scattering (1/cm)
0	0
.14	-0.02
.28	-0.04
.56	-0.07
1.12	-0.15
2.23	-0.34
4.46	-0.90

In initial cavity designs, the observed increase in absorption at high concentrations of scatterers was attributed to creation of an anisotropy of the F_0 irradiance at the sample surface by the S_0 detector fiber. Specifically, the fiber is a radiation sink so the radiation density in its immediate vicinity is decreased. The cavity design of models II - IV were intended to decrease this effect; the F_0 irradiance is allowed to travel down a Spectralon tunnel where a fiber can sample the intensity without directly contacting the sample. The anisotropy caused by the detector will be averaged over the larger entrance area of this tunnel. The experimental results have shown that this was in fact not a major source of the problem. Each of the design modifications of models II - IV produced the same response as shown in figure 14.

Based on an analytic one-dimensional model developed by Dr. G. W. Kattawar[18], we now believe that the apparent increase in absorption in the presence of a high concentration of particles is due to an anisotropy of the radiation density in the sample. Specifically, the scattering is so great that even with very weak absorption, the center of the sample is darker than the region close to the Spectralon wall. The scattering increases the effective path length through the sample. The effective path length from the sample boundary to the sample midpoint becomes long enough for the absorption of the medium (water in this case) to appreciably decrease the radiance in the center of the sample. Figure 15 shows the irradiance as a function of the fractional distance from the sample boundary to the center of the sample for a sample with an optical depth of .53 and a cavity with dimensions of model II (based on Dr Kattawar's one dimensional model of an ICAM). This effect will be dependent on the concentration of scatterers, the absorption of the sample, and on the diameter of the sample cell. If we increase the cell diameter we expect to see this same effect at a lower concentration of scatterers. Figure 14 shows the effect of increasing concentrations of scatterers suspended in water for model II (cell diameter of 3.7 cm) and for model V (cell diameter of 9 cm). The absorption begins to increase at a lower concentration of scatterers as the cell diameter increases.

This means that at extremely high concentrations of scatterers our assumption of a isotropic, homogeneous radiance distribution in the sample volume is no longer valid. Specifically the term for the energy absorbed in equation (1) is no longer valid at these high

concentrations of scatterers (F_0 is not constant throughout the sample volume). This does not, however, significantly limit the use of the ICAM as these concentrations of scatterers are far greater than what would normally be encountered. In cases where it is necessary to measure absorption in the presence of such high concentrations of scatterers, an ICAM with a smaller sample volume should be used.

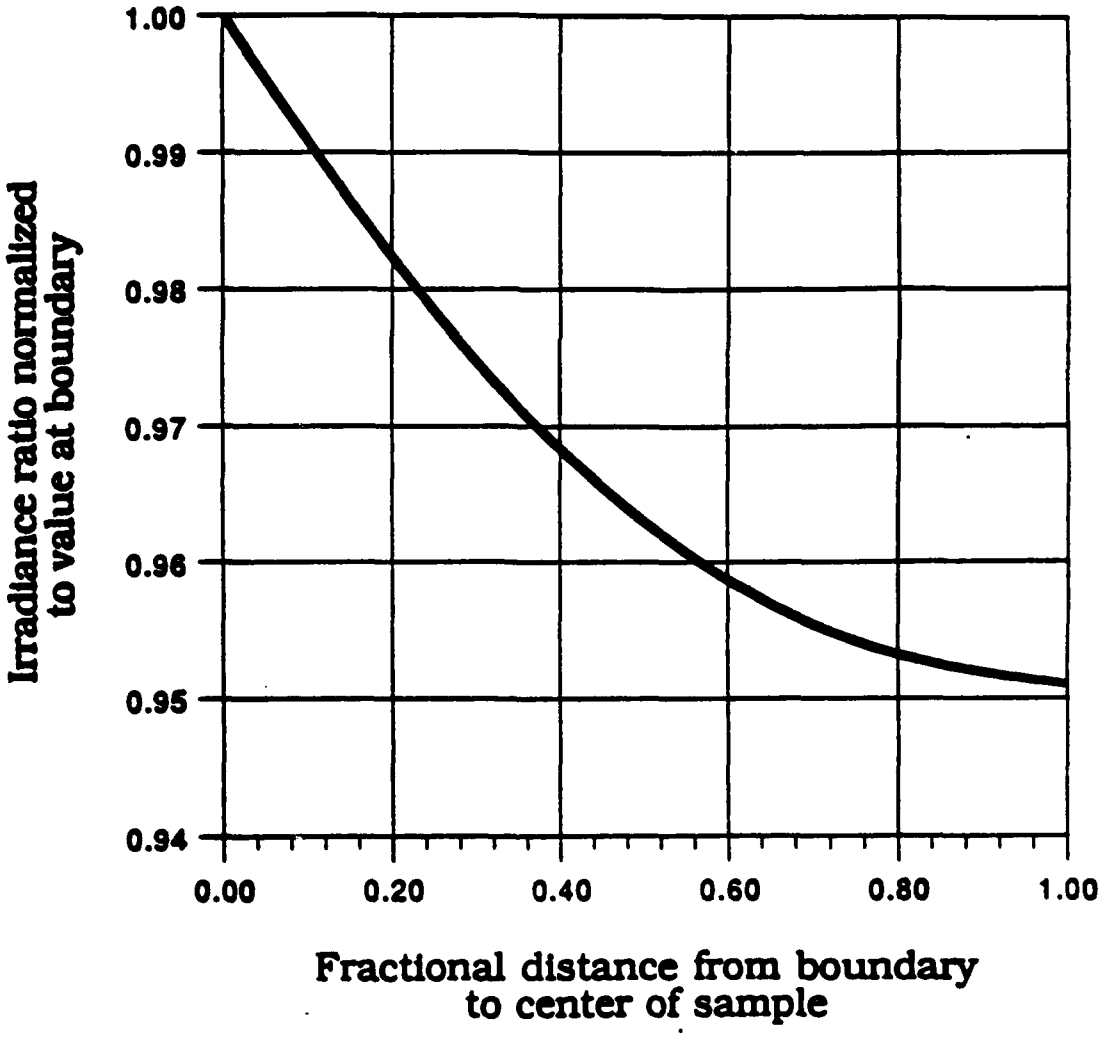

Figure 15. Irradiance vs distance from sample boundary.

B. Linearity

Linearity of the ICAM was tested by measuring the absorption coefficient for a series of dye solutions containing incremental amounts of pigment dissolved in filtered/deionized water. As shown in figure 16, the data remained linear up to an absorption of 25 meter^{-1} for model II. Models III and IV were found to become nonlinear at much lower concentrations of dye than models where the quartz cell completely filled the diameter of the inner cavity. This result is not yet fully understood.

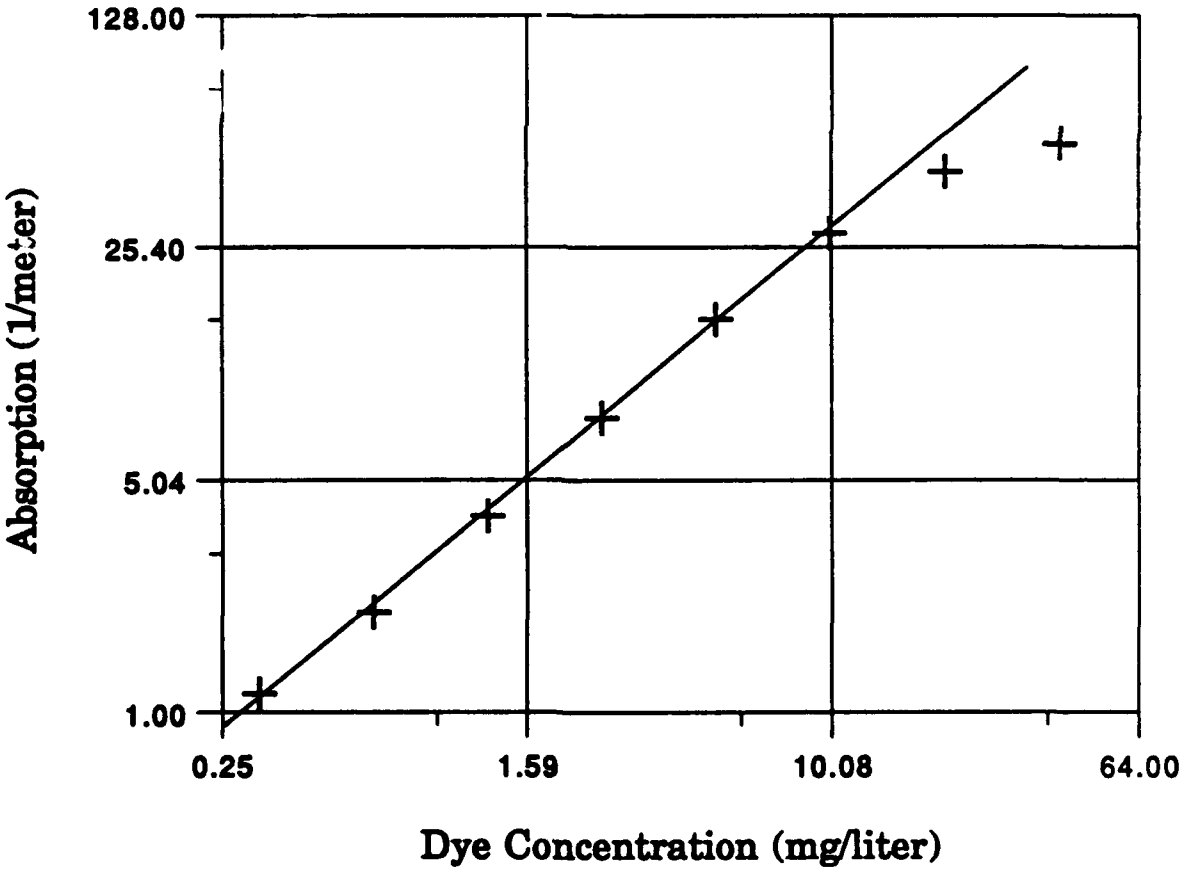

Figure 16. Linearity test; absorption versus dye concentration.

Model V remained linear up to an absorption of 15 meter^{-1}. As the dimensions of the cavity are increased a nonlinear result is expected at lower concentrations of dye due to the longer path length through the absorber. This result indicates that accurate calibration constants can be obtained only by calibrating with samples which avoid the nonlinear region.

C. Spectral Measurements

Models II and V have been used to measure absorption spectra of pure and natural waters and of phytoplankton cultures. In August of 1989, model II was used to measure various samples at the Naval Oceanographic Research and Development Agency located at Stennis Space Center, Mississippi. At this time a method for determining the calibration constant K_2 without reference to accepted values for absorption of pure water had not been realized. Since the cavity was known to measure total absorption, data from Smith and Baker[2] for the absorption of pure water was added to the absorption of calibration samples measured in a spectrophotometer. This allowed us to plot total absorption vs S_1/S_0, and to determine both K_1 and K_2 from this data as described previously. This would introduce an error in our measurements equal to the uncertainty of the Smith and Baker data for absorption of pure water. This uncertainty would be negligible for any absorption significantly greater than that of pure water but would become significant for very small absorptions. Figures 17 through 21 reflect data taken after calibration using this method. Figure 17 shows the absorption spectra of distilled water as

well as seawater and filtered seawater taken from the Gulf of Mexico. The difference between the seawater and the seawater filtrate spectra is shown in figure 18 and indicates a typical absorption spectra for marine phytoplankton (the primary suspended particulate found in seawater). Figure 19 shows the difference between the spectra of the seawater filtrate and distilled water and is typical of a spectra for dissolved organic matter. Figure 20 shows the spectra for a laboratory culture of phytoplankton known as *Dunaliella tertiolecta*. The difference between the spectra for the sample and the filtrate gives the absorption of the phytoplankton. To examine the sensitivity of the ICAM, a laboratory culture of *Micromonas pusilla* was diluted to obtain a concentration of chlorophyll-a of only 0.44 mg per cubic meter (within the range of the purest natural waters). The difference in absorption between the sample and the filtrate was on the order of only .001 meters^{-1}, yet the ICAM could resolve the characteristic spectra for this phytoplankton species as shown in figure 21. The fact that this spectra compares favorably to the spectra for the same species measured in a spectrophotometer using other methods indicates that calibration errors due to the uncertainty of the Smith and Baker data for pure water is negligible. Between 400 to 490 nm the spectrophotometer data is abnormally high. The spectrophotometer data also shows an error in the shape of the curve between 400 and 420 nm. The absorption maximum should be at 420 nm not at 400 nm. This is attributed to some procedural or systematic error in the spectrophotometer data[19].

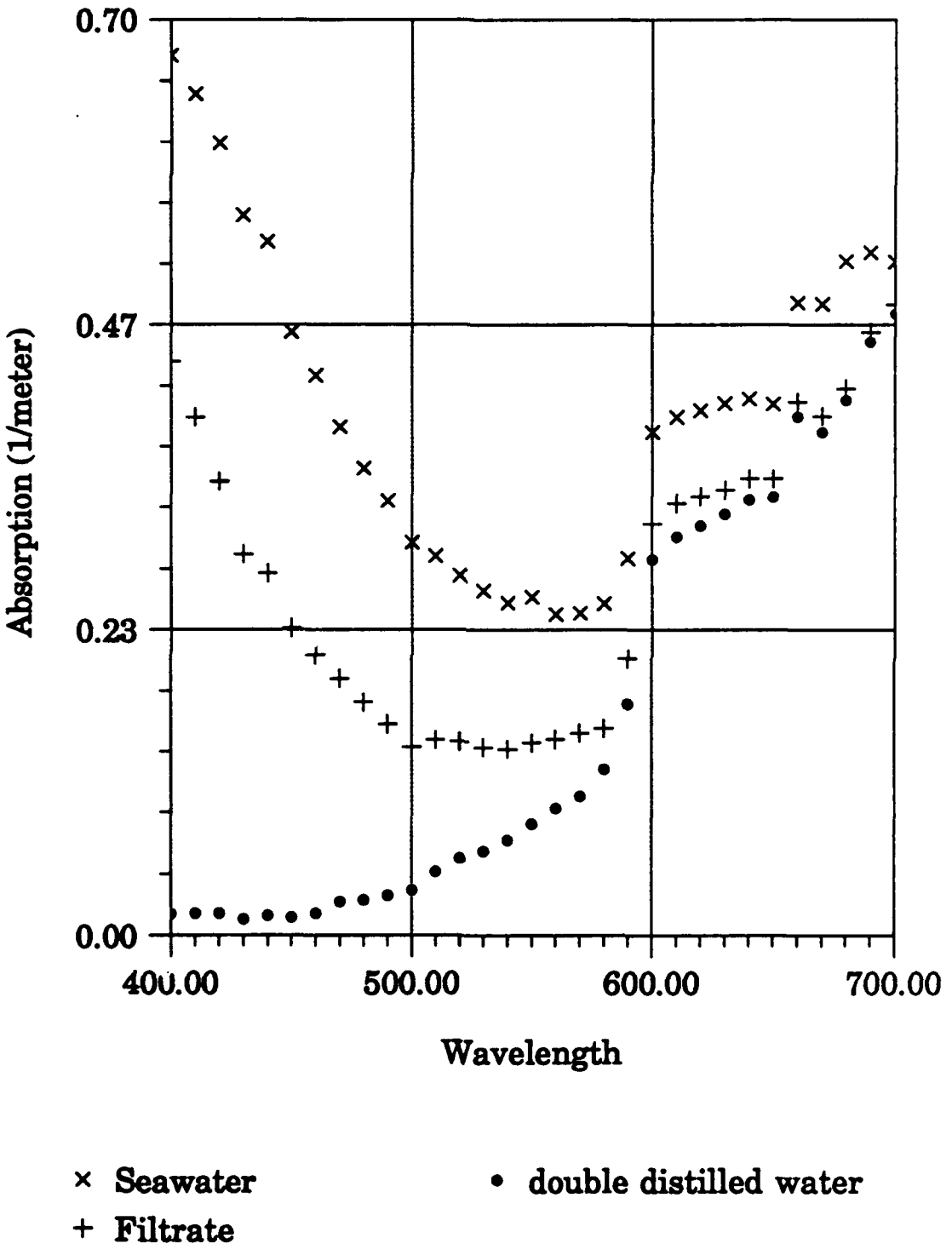

Figure 17. Absorption spectra for seawater, seawater filtrate, and distilled water.

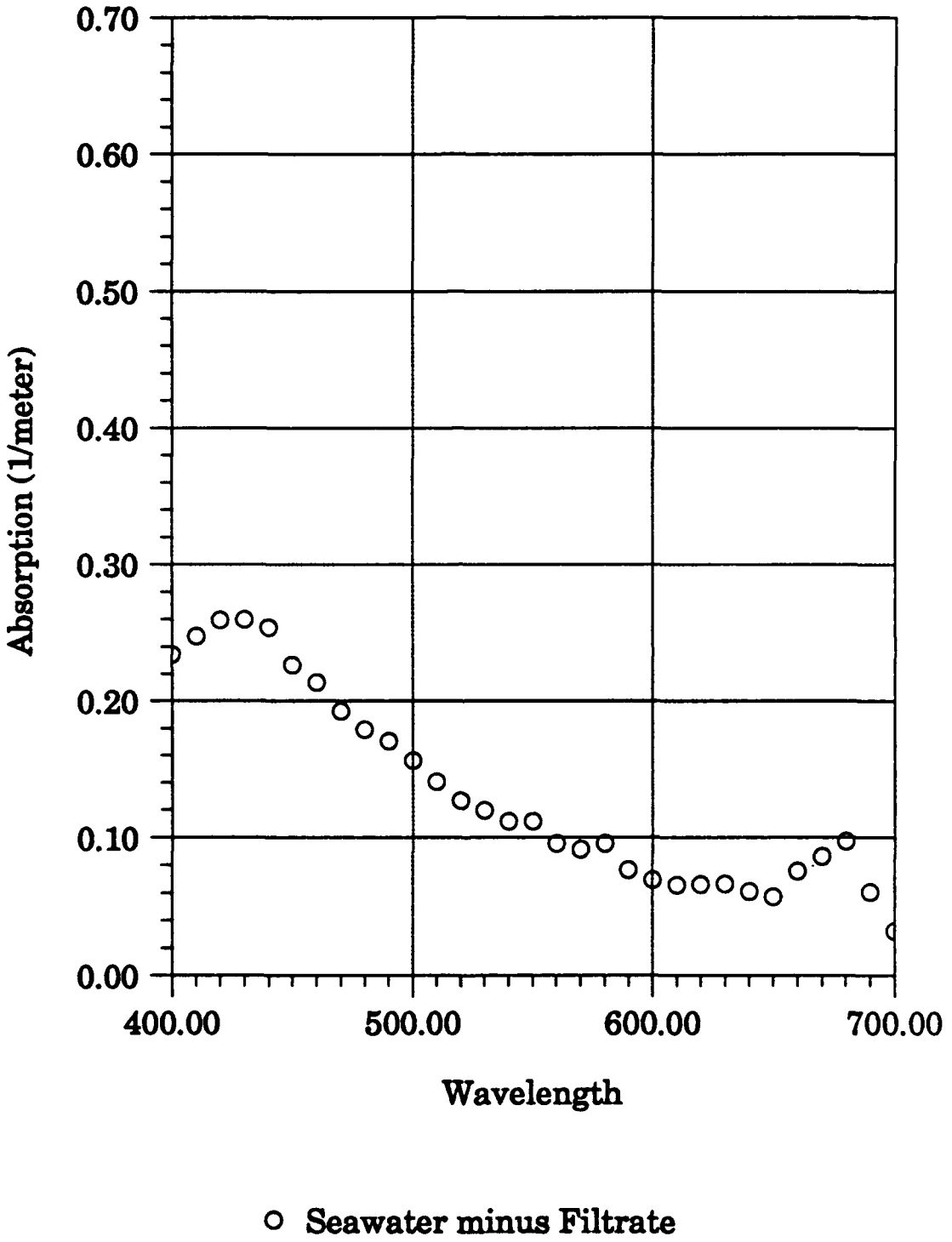

Figure 18. Absorption spectra for seawater particulates.

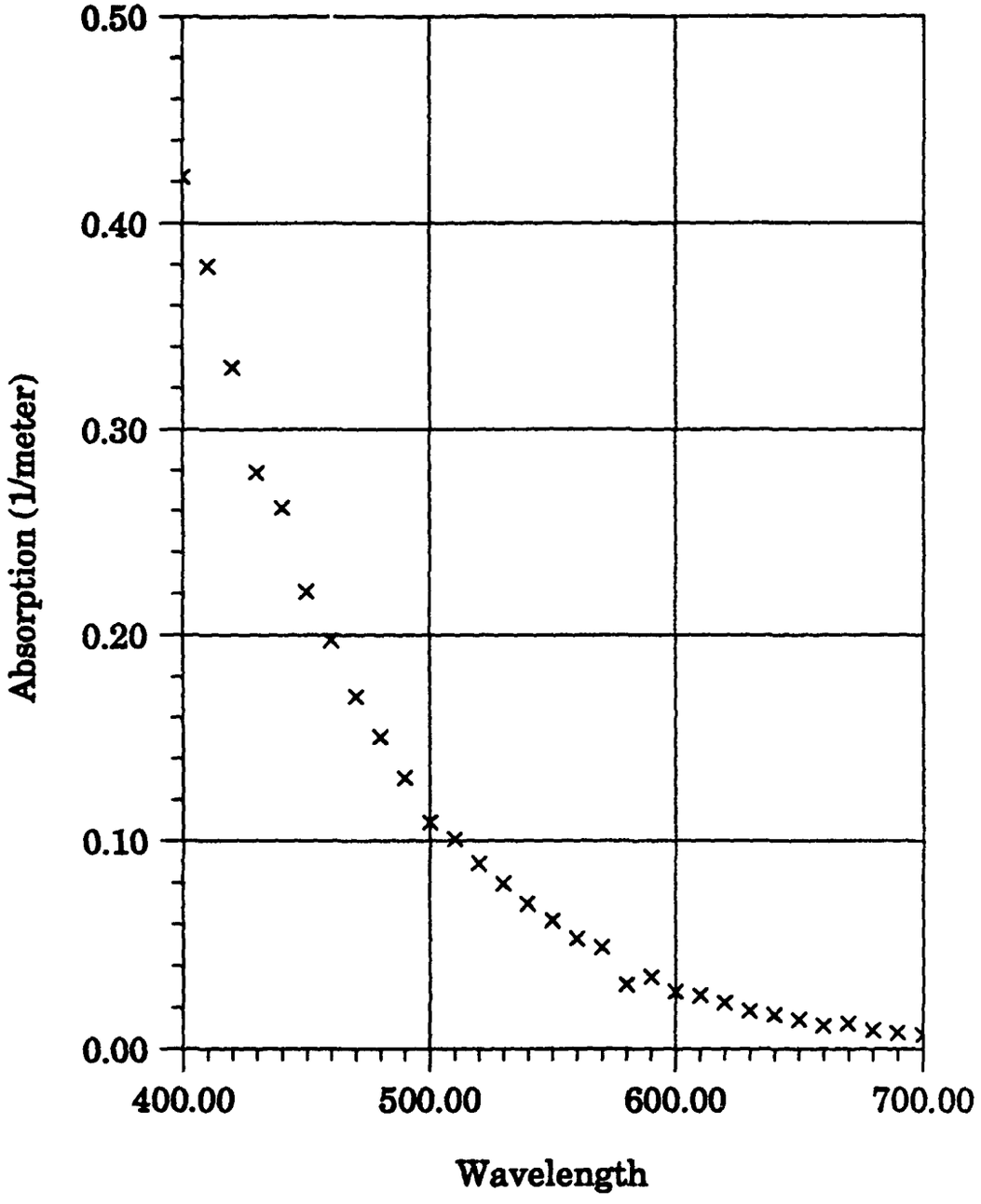

Figure 19. Difference between seawater filtrate and distilled water.

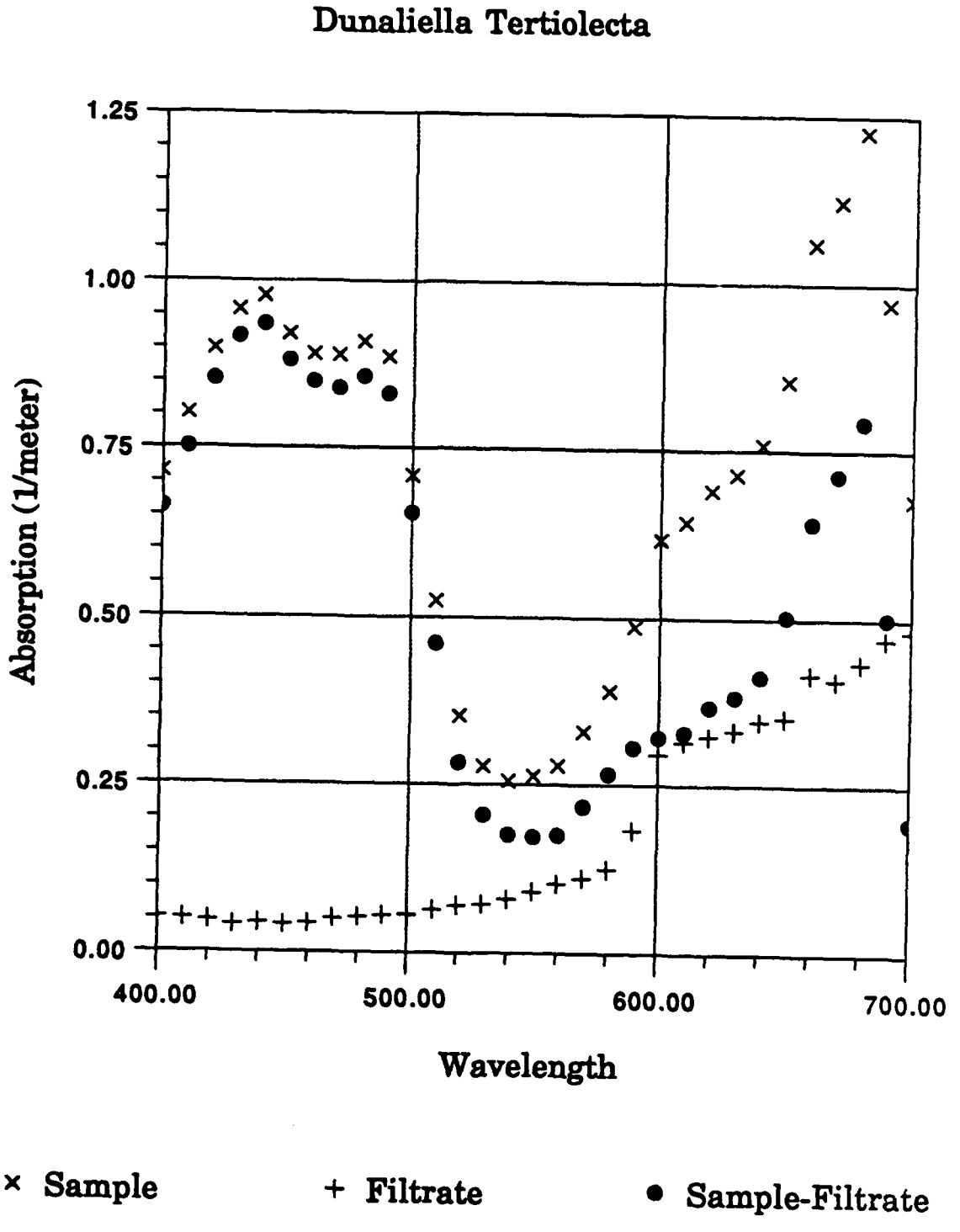

Figure 20. Absorption spectra for *Dunaliella tertiolecta.*

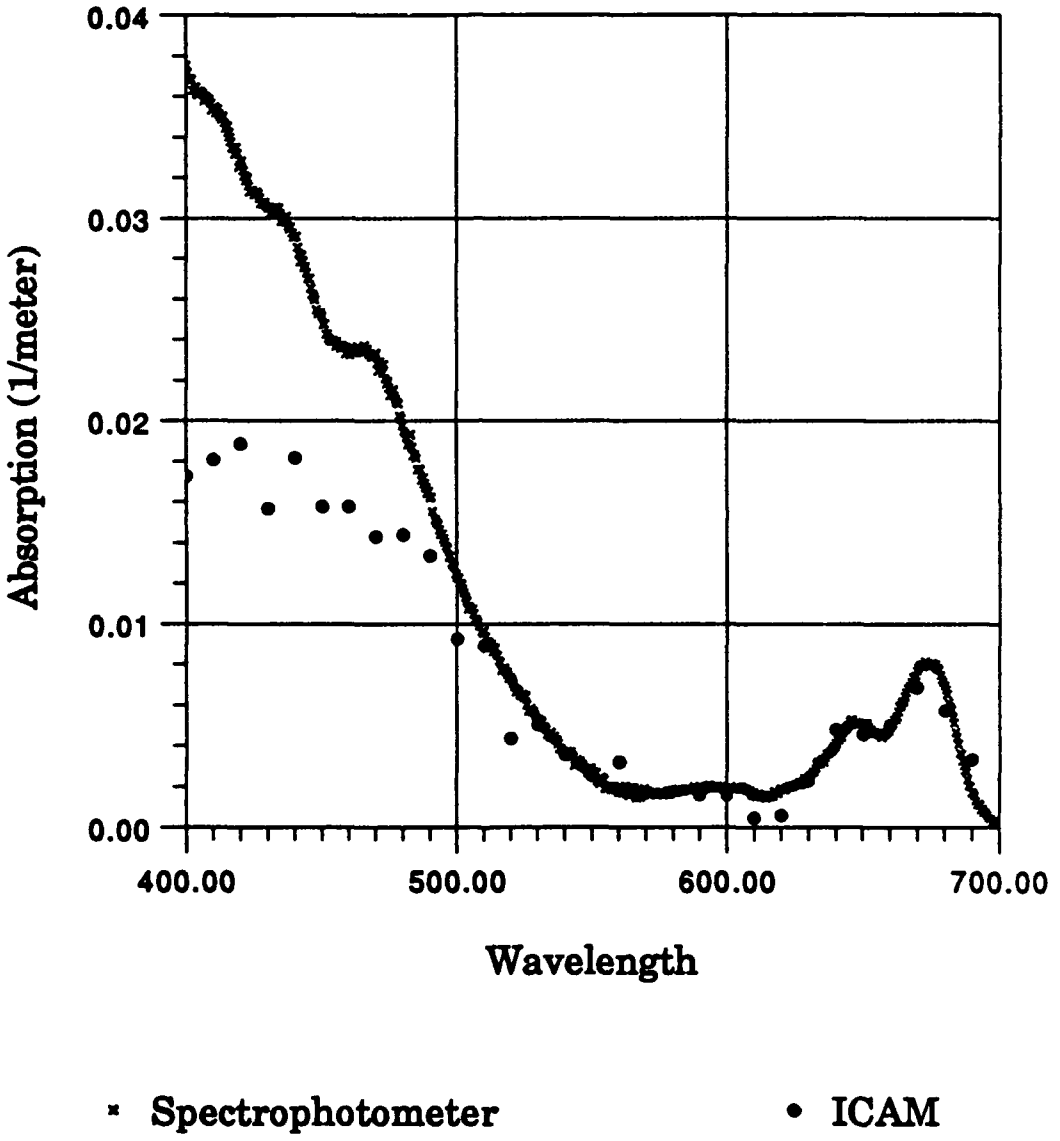

Figure 21. Absorption spectra for *Micromonas pusilla.*

Model V of the ICAM was completed in December of 1989. Calibration was accomplished using the method where K_2 is determined by setting the absorption equal to zero with the cavity empty. Figures 22 and 23 show a comparison of several pure water samples with the data from Smith and Baker. Three samples of filtered-deionized water and one sample each of HPLC grade water and seawater were measured at various times over a four day period.

The spectra agree well in the wavelength region from 550 to 700 nm with the exception of the points at 660, 680, 690, and 700. This discrepancy is attributed to the following calibration error. The absorption spectra for calibration sample 1 (shown in figure 11) appears discontinuous at 660 and 680 nm and the absorptions of all three samples vary by less than .006 meters^{-1} from 690 to 700 nm which would allow greater error in determining K_1 in this region.

In the region from 460 to 550 nm the ICAM data were consistent in that the spectra for three different samples of deionized-filtered water and HPLC grade water measured at different times over a 4 day period all agree to within an absorption value of .01 meters^{-1}. The absorption of the seawater sample is consistent with the other samples in this region in that the values agree at the higher wavelengths and the absorption of the seawater sample slowly increases as the wavelength decreases, indicating some dissolved organics in the seawater sample. Even though the ICAM data is consistent in this region it is less than the data of Smith and Baker and reaches negative absorption values from 460 to 490 nm which we know to be erroneous. This error has not yet been identified but may

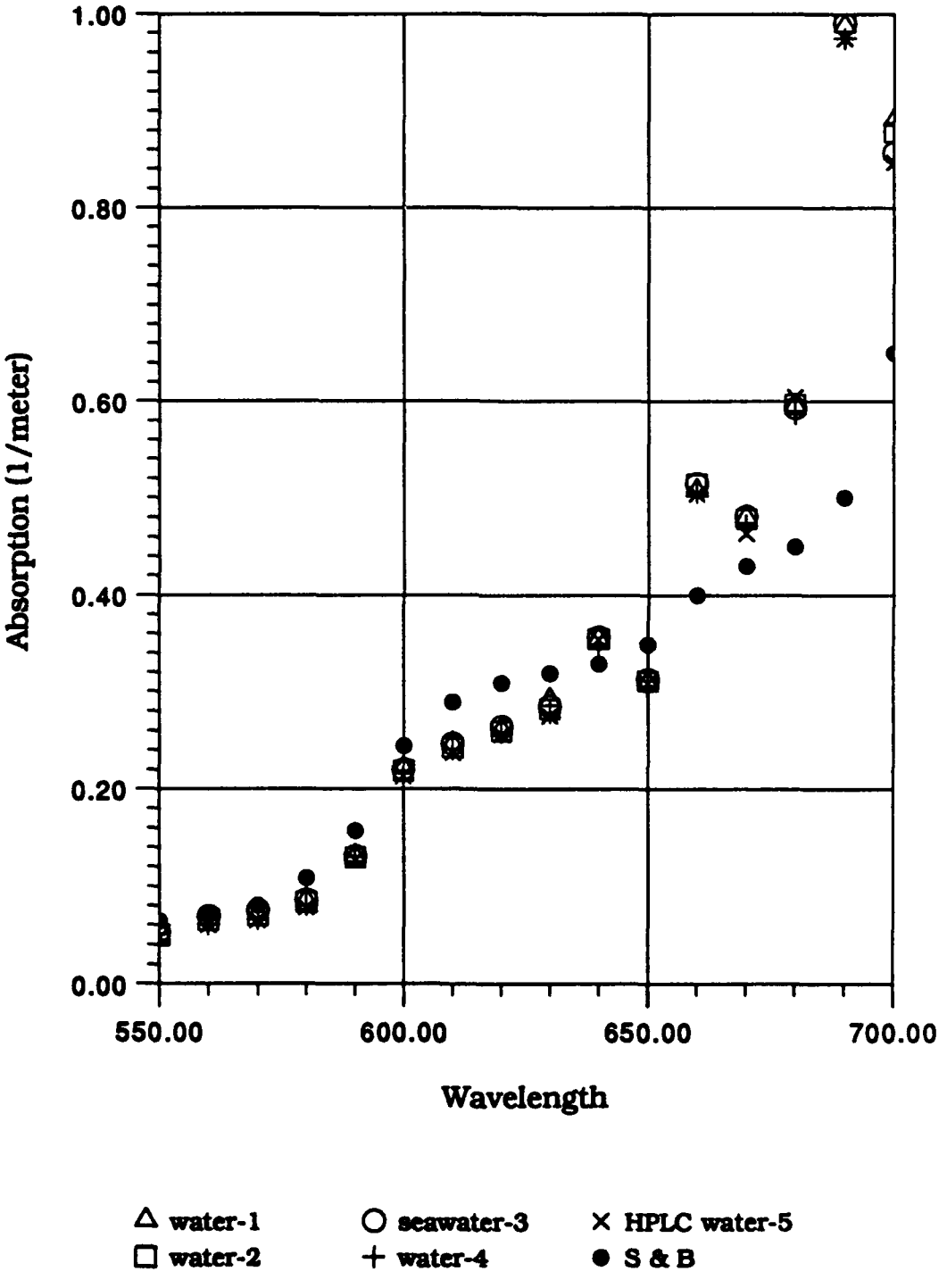

Figure 22. Absorption spectra for various pure waters compared to data from Smith and Baker, 550 to 700 nm.

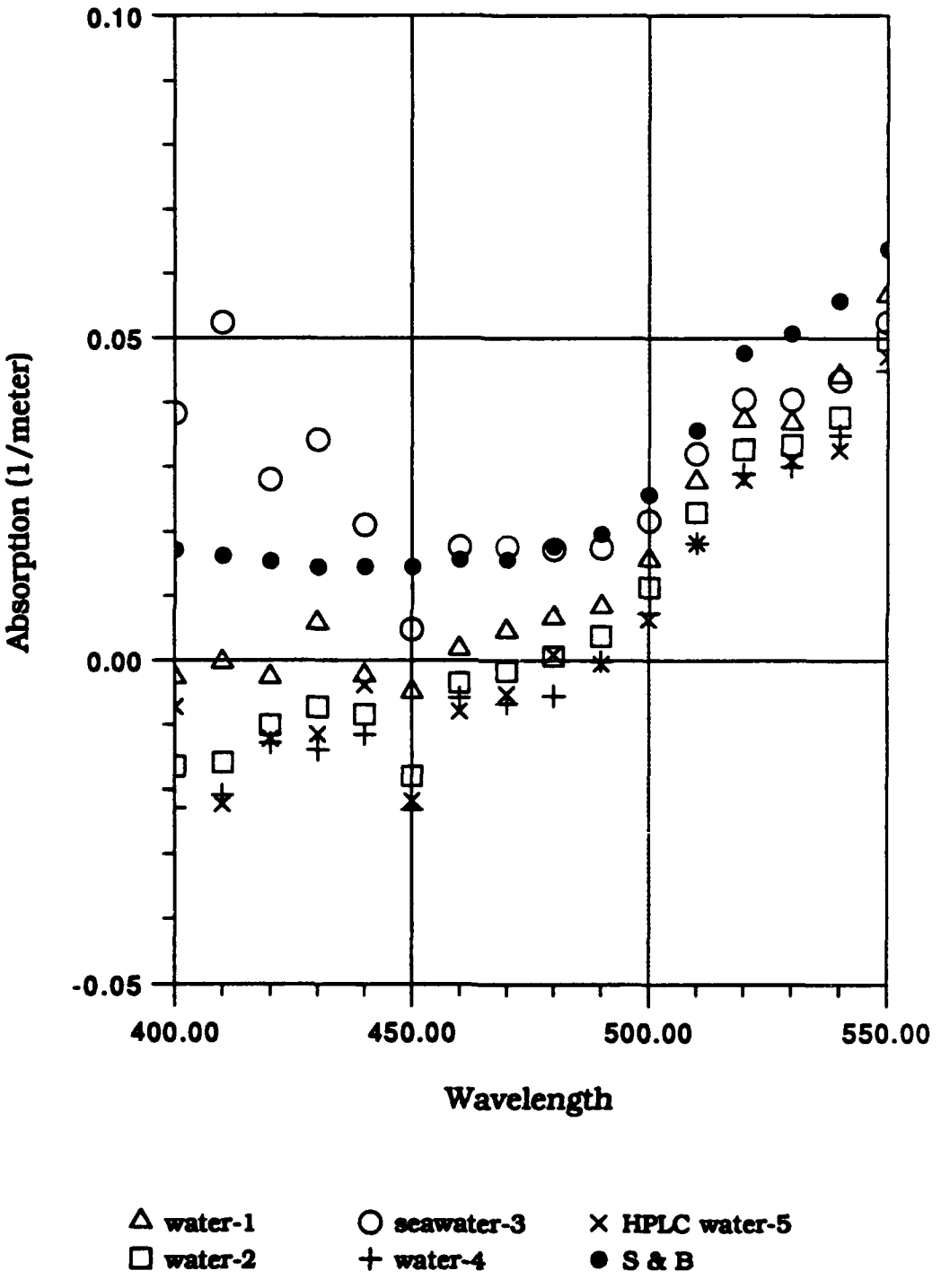

Figure 23. Absorption spectra for various pure waters compared to data from Smith and Baker, 400 to 550 nm.

be due to several causes. It may be attributed to calibration errors due the change in the refractive index between the cavity empty and filled with water. Specifically, determining the calibration constant K_2 by setting the absorption equal to zero with the cavity empty assumes no appreciable change in the optical properties of the cavity between the cavity when filled with air and water. This error may also be attributed to contamination of the sample cell. If the Irgalan Black solutions used for calibration leave a slight residue on the quartz cell, then the measurement of S_1/S_0 with the cell empty would be higher than if this contamination were not present. This would not affect our measurements as long as the contamination remained constant. If, however, the contamination is subsequently removed due to repeated rinsing of the sample cell, then all values for S_1/S_0 and absorption would decrease by a value equal to the absorption of the contamination that was removed. This implies a change in the intercept, K_2, of equation (3). If this change is extremely small it would only become significant when measuring the smallest absorption coefficients. Since the absorption of pure water drops by an order of magnitude as the wavelength falls below 550 nm, it is conceivable that the effect would show up here. Furthermore, if some contamination were being removed each time the sample cell was rinsed, then each successive measurement would indicate a lower absorption as more and more of the contamination was removed. The number following each sample identification in the legend of figure 23 indicates the sequence in which the samples were measured.

Since successive samples of the filtered deionized water show decreasing absorption values, this is a very likely possibility.

In the region from 400 to 450 nm the absorption values of similar samples varied by as much as .02 meters^{-1}, and were also negative. The negative values are attributed to the same error as discussed for the region from 460 to 500 nm. The variance in the values is attributed to noise of the lock-in amplifier. Specifically, the gain for the S_0 signal in this region is 4 to 10 times that used for the rest of the spectrum. The absorption values in this region are also an order of magnitude smaller than those in the rest of the spectrum. This leads to comparatively more noise in the absorption values, and indicates that data should be averaged over a longer time period when operating in the lower wavelength region.

C. Energy Density Within the Sample

For many absorption measurements it is desirable to know the intensity of the radiation striking the sample. One example of this is in measuring the absorption of phytoplankton. Absorption can be affected if the incident radiation photoinhibits the phytoplankton.

We denote the scalar radiance at a point within the cavity sample volume as $L(\vec{r},\hat{\Omega})$ and assume that it is uniform and isotropic,

$$L(\vec{r},\hat{\Omega}) = L_0 = \text{constant}\,\frac{\text{watts}}{\text{m}^2\cdot\text{steradians}}\,.$$

In the cavity the radiant flux incident on the detector fiber from within a solid angle $\Delta\Omega$ will be,

$$P = L_0\Delta\Omega A,$$

where A is the fiber area. The portion of this power that enters the fiber is a function of the angle of incidence at the fiber end. We will denote the fiber acceptance function as $g(\theta)$ where θ is the angle between the incident radiation and the fiber axis. The power in the fiber will then be $Pg(\theta)$ giving a signal

$$\begin{aligned} S_0 &= K\int P\cdot g(\theta), \\ &= KL_0A\int_{\Omega} g(\theta)\cdot d\Omega, \\ &= KL_0A2\pi\int_{\theta} g(\theta)\cdot \sin(\theta)\cdot d\theta, \end{aligned} \tag{5}$$

where K is a constant which converts the optical signal into units of volts. We want to find L_0, and solving equation (5) for it, we obtain

$$L_0 = \frac{S_0}{2\pi A\int_{\theta} K\cdot g(\theta)\cdot \sin(\theta)\cdot d\theta}.$$

We experimentally determine $Kg(\theta)$ using the experimental apparatus shown in figure 24. The S_0 detector fiber, coupled to its photomultiplier tube, was removed from the cavity and mounted on a rotational platform with the detector end of the fiber positioned at the center of rotation. A HeNe laser of known beam power was used as a source. The laser beam was directed at the S_0 fiber and passed through a neutral density filter and then through a light chopper and focusing lens. Values for S_0 were recorded every 2.5 degrees as the S_0 detector fiber was rotated through 180 degrees with respect to the incident laser beam. This produced values for S_0 as a function of the angle of incidence of the light source which we call $S_r(\theta)$. We assume the acceptance of the fiber is rotationally symmetric about the fiber axis. The power incident on the fiber is P_L, the laser power

after passing through the neutral density filter and the light chopper. The portion that enters the fiber is $P_L \cdot g(\theta)$ which gives a signal

$$S_F(\theta) = K \cdot P_L \cdot g(\theta),$$

or

$$K \cdot g(\theta) = \frac{S_F(\theta)}{P_L} .$$

Substituting this into the equation for L_0 gives

$$L_0 = \frac{S_0 \cdot P_L}{4\pi A \int_0^{\pi/2} S_F(\theta) \cdot \sin(\theta) \cdot d\theta} ,$$

we numerically integrate the $S_F(\theta)$ data.

$$\int_0^{\pi/2} S_F(\theta) \cdot \sin(\theta) \cdot d\theta = C,$$

to find

$$L_0 = \frac{S_0 \cdot P_L}{4\pi AC} .$$

The irradiance normal to any surface in the cavity is

$$F_0 = \pi L_0 = \frac{P_L}{4AC} \cdot S_0 .$$

For a wavelength of 628 nm and using the detector fiber from model V, the value for L_0 is .048 watts/$m^2 \cdot sr$. The energy density (U) is just

$$U = 4\pi L_0 m/c$$

where m is the index of refraction and c is the speed of light.

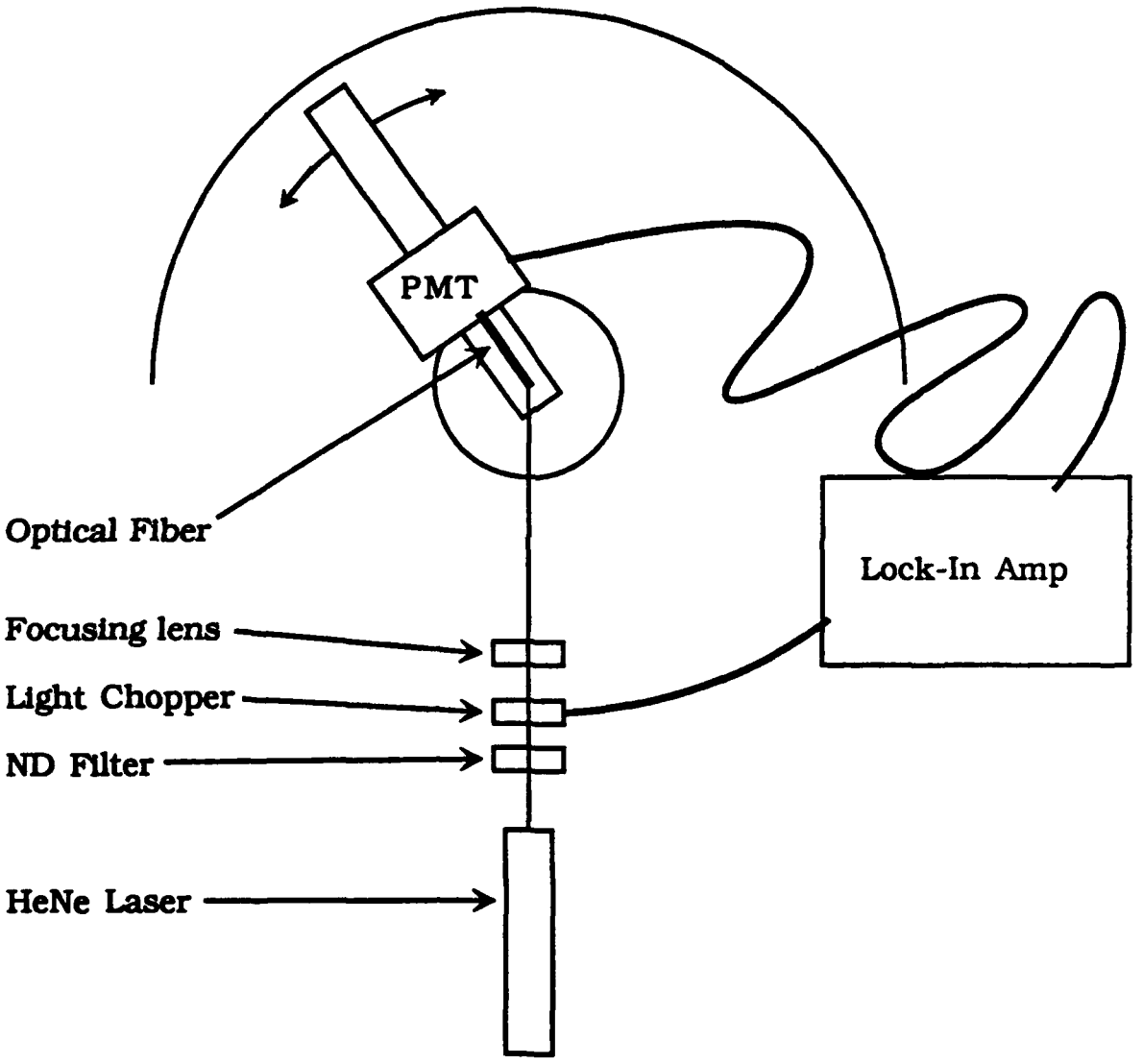

Figure 24. Experimental apparatus to determine $Kg(\theta)$.

CHAPTER VII

CONCLUSION

The ICAM has been shown to be capable of measuring absorption independent of scattering. It can be used to accurately measure very small absorptions (less than .005 meters^{-1}) and to measure the absorption of suspended particulate matter.

There are still some residual problems such as identification and correction of the error that produced negative absorption values for pure water in the lower wavelength region, which will be studied in future work.

REFERENCES

[1] E. S. Fry and G. W. Kattawar, "Measurement of the Absorption Coefficient of Ocean Water Using Isotropic Illumination," Proc. SPIE **925**, Ocean Optics IX, 142-148 (1988).

[2] Raymond C. Smith and Karen S. Baker, "Optical Properties of the Clearest Natural Waters (200-800 nm),"Appl. Opt. vol. 20, no. 2, 177-184 (1981).

[3] L. H. Dawson and E. O. Hulburt, "The Absorption of Ultraviolet and Visible Light By Water," Journal Optical Society of America **24**, 175-177 (1934).

[4] E. O. Hulburt, "Optics of Distilled and Natural Water," Journal of the Optical Society of America **35**, 698-705 (1945).

[5] H. R. James, and E. A. Birge, "A Laboratory Study of the Absorption of Light by Lake Water," Wisc. Acad. Sci. Trans. **31**, 1-154 (1938).

[6] C. S. Yentsch, "Measurement of Visible Light Absorption by Particulate Matter in the Ocean," Limnology and Oceanography **7**, 207-217 (1962).

[7] G. D. Gilbert, R. C., Honey, R. E. Myers, and G. P. Sorenson, Optical Absorption Meter, (Stanford Research Inst., Menlo Park, Ca., 1969).

[8] John T. O. Kirk, Light and Photosynthesis in Aquatic Ecosystems, (Cambridge U.P., New York, 1983).

[9] J. Stone, "Measurements of the Absorption of Light in Low-Loss Liquids," Journal of the Optical Society of America **62**, 327-333 (1972).

[10] Marvin Hass, James W. Davidson, Herbert B. Rosenstock, and Julius Babiskin, "Measurement of Very Low Absorption Coefficients by Laser Calorimetry," Appl. Opt. **14**, 1128-1130 (1975).

[11] M. R. Querry, P. G. Cary, and R. C. Waring, "Split-pulse Laser Method for Measuring Attenuation Coefficients of Transparent Liquids: Application to Deionized Filtered Water in the Visible Region," Appl. Opt. **17**, 3587-3592 (1978).

[12] A. C. Tam and C. K. N. Patel, "Optical Absorptions of Light and Heavy Water by Laser Optoacoustic Spectroscopy," Appl. Opt. **18**, 3348-3358 (1979).

[13] P. Elterman, "Integrating Cavity Spectroscopy," Appl. Opt. **9**, 2141-2142 (1970).

[14] A. M. Emel'yanov, V. I. Kosyakov, and B. V. Makushkin, "The Use of an Integrating Cavity for Measuring Small Optical Absorptions," Soviet Journal of Optical Technology **45**, 31-33 (1978).

[15] H. Maske and H. Haardt, "Quantitative *in vivo* absorption spectra of phytoplankton: Detrital absorption and comparison with florescence excitation spectra," Limnology and Oceanography **32**, 620-633 (1987).

[16] K. Fischer, "Measurements of Absorption of Visible Radiation by Aerosol Particles," Beiträge zur Physik der Atmosphäre, **43**, 244-254 (1970).

[17] Antony D. Clarke, "Integrating sandwich: a new method of measurement of the light absorption coefficient for atmospheric particles," Appl. Opt., **21**, 3011-3020 (1982).

[18] G. W. Kattawar, Department of Physics, Texas A&M University, College Station, Texas (personal communication 1989).

[19] Joan Cleveland, *NOARL, Stennis Space Center, Mississippi* (personal communication 1989).

VITA

Captain Robin Merl Pope received a B.S. degree from the United States Military Academy in June of 1979 and was commissioned as a Second Lieutenant in the United States Army. After serving in various command and staff assignments he was selected to participate in the Army's advanced degree program. His permanent mailing address is:

3949 Fairfax Drive

Chattanooga, Tennessee 37415.